

Durham Research Online

Deposited in DRO:

19 August 2014

Version of attached file:

Other

Peer-review status of attached file:

Peer-reviewed

Citation for published item:

Ó Cofaigh, C. and Davies, B.J. and Livingstone, S.J. and Smith, J.A. and Johnson, J.S. and Hocking, E.P. and Hodgson, D.A. and Anderson, J.B. and Bentley, M.J. and Canals, M. and Domack, E. and Dowdeswell, J.A. and Evans, J. and Glasser, N.F. and Hillenbrand, C.D. and Larter, R.D. and Roberts, S.J. and Simms, A.R. (2014) 'Reconstruction of ice-sheet changes in the Antarctic Peninsula since the Last Glacial Maximum.', *Quaternary science reviews.*, 100 . pp. 87-110.

Further information on publisher's website:

<http://dx.doi.org/10.1016/j.quascirev.2014.06.023>

Publisher's copyright statement:

© 2014 Durham University. Published by Elsevier Ltd. This is an open access article under the CC BY license (<http://creativecommons.org/licenses/by/3.0/>).

Additional information:

Use policy

The full-text may be used and/or reproduced, and given to third parties in any format or medium, without prior permission or charge, for personal research or study, educational, or not-for-profit purposes provided that:

- a full bibliographic reference is made to the original source
- a [link](#) is made to the metadata record in DRO
- the full-text is not changed in any way

The full-text must not be sold in any format or medium without the formal permission of the copyright holders.

Please consult the [full DRO policy](#) for further details.



Contents lists available at ScienceDirect

Quaternary Science Reviews

journal homepage: www.elsevier.com/locate/quascirev

Reconstruction of ice-sheet changes in the Antarctic Peninsula since the Last Glacial Maximum

Colm Ó Cofaigh ^{a,*}, Bethan J. Davies ^{b,1}, Stephen J. Livingstone ^c, James A. Smith ^d,
Joanne S. Johnson ^d, Emma P. Hocking ^e, Dominic A. Hodgson ^d, John B. Anderson ^f,
Michael J. Bentley ^a, Miquel Canals ^g, Eugene Domack ^h, Julian A. Dowdeswell ⁱ,
Jeffrey Evans ^j, Neil F. Glasser ^b, Claus-Dieter Hillenbrand ^d, Robert D. Larter ^d,
Stephen J. Roberts ^d, Alexander R. Simms ^k

^a Department of Geography, Durham University, Durham, DH1 3LE, UK^b Centre for Glaciology, Department of Geography and Earth Sciences, Aberystwyth University, Aberystwyth, SY23 3DB, Wales, UK^c Department of Geography, University of Sheffield, Sheffield, S10 2TN, UK^d British Antarctic Survey, High Cross, Madingley Road, Cambridge, CB3 0ET, UK^e Department of Geography, Northumbria University, Newcastle upon Tyne, NE1 8ST, UK^f Department of Earth Sciences, Rice University, 6100 Main Street, Houston, TX, USA^g CRG Marine Geosciences, Department of Stratigraphy, Paleontology and Marine Geosciences, Faculty of Geology, University Barcelona, Campus de Pedralbes, C/Marti i Franques s/n, 08028, Barcelona, Spain^h College of Marine Science, University of South Florida, 140 7th Avenue South, St. Petersburg, FL 33701-5016, USAⁱ Scott Polar Research Institute, University of Cambridge, Cambridge, CB2 1ER, UK^j Department of Geography, University of Loughborough, Loughborough, LE11 3TU, UK^k Department of Earth Science, University of California, Santa Barbara, 1006 Webb Hall, Santa Barbara, CA, 93106, USA

ARTICLE INFO

Article history:

Received 26 September 2013

Received in revised form

11 June 2014

Accepted 18 June 2014

Available online xxx

Keywords:

Antarctic Peninsula Ice Sheet

Last Glacial Maximum

Deglaciation

Antarctica

Glacial geology

ABSTRACT

This paper compiles and reviews marine and terrestrial data constraining the dimensions and configuration of the Antarctic Peninsula Ice Sheet (APIS) from the Last Glacial Maximum (LGM) through deglaciation to the present day. These data are used to reconstruct grounding-line retreat in 5 ka time-steps from 25 ka BP to present. Glacial landforms and subglacial tills on the eastern and western Antarctic Peninsula (AP) shelf indicate that the APIS was grounded to the outer shelf/shelf edge at the LGM and contained a series of fast-flowing ice streams that drained along cross-shelf bathymetric troughs. The ice sheet was grounded at the shelf edge until ~20 cal ka BP. Chronological control on retreat is provided by radiocarbon dates on glaci-marine sediments from the shelf troughs and on lacustrine and terrestrial organic remains, as well as cosmogenic nuclide dates on erratics and ice moulded bedrock. Retreat in the east was underway by about 18 cal ka BP. The earliest dates on recession in the west are from Bransfield Basin where recession was underway by 17.5 cal ka BP. Ice streams were active during deglaciation at least until the ice sheet had pulled back to the mid-shelf. The timing of initial retreat decreased progressively southwards along the western AP shelf; the large ice stream in Marguerite Trough may have remained grounded at the shelf edge until about 14 cal ka BP, although terrestrial cosmogenic nuclide ages indicate that thinning had commenced by 18 ka BP. Between 15 and 10 cal ka BP the APIS underwent significant recession along the western AP margin, although retreat between individual troughs was asynchronous. Ice in Marguerite Trough may have still been grounded on the mid-shelf at 10 cal ka BP. In the Larsen-A region the transition from grounded to floating ice was established by 10.7–10.6 cal ka BP. The APIS had retreated towards its present configuration in the western AP by the mid-Holocene but on the eastern peninsula may have approached its present configuration several thousand years earlier, by the start of the Holocene. Mid to late-Holocene retreat was diachronous with stillstands, re-advances and changes in ice-shelf configuration being recorded in most places. Subglacial

* Corresponding author. Tel.: +44 1913341890; fax: +44 1913341801.

E-mail address: colm.ocofaigh@durham.ac.uk (C. Ó Cofaigh).¹ Now at: Centre for Quaternary Research, Department of Geography, Royal Holloway, University of London, Surrey, TW20 0EX, UK.

topography exerted a major control on grounding-line retreat with grounding-zone wedges, and thus by inference slow-downs or stillstands in the retreat of the grounding line, occurring in some cases on reverse bed slopes.

© 2014 The Authors. Published by Elsevier Ltd. This is an open access article under the CC BY license (<http://creativecommons.org/licenses/by/3.0/>).

1. Introduction

The Antarctic Peninsula (AP) (Fig. 1) is arguably the most intensively studied region in Antarctica. This reflects its climatic sensitivity and recognition that it is one of the most rapidly warming areas of the globe today (Vaughan et al., 2003; Turner et al., 2005; Bentley et al., 2009). This warming is indicated by a range of observations, but perhaps most dramatically, is manifest in the collapse of ice shelves fringing the Peninsula (e.g., Vaughan and Doake, 1996; Scambos et al., 2003), and in the thinning, retreat and acceleration of marine-terminating outlet glaciers over the last few decades (De Angelis and Skvarca, 2003; Cook et al., 2005).

Understanding of the longer-term Quaternary glacial history of the AP has seen significant advances in the last 20 years, due particularly to technological developments in offshore marine geophysical surveying and terrestrial dating techniques. This has allowed detailed reconstruction of former ice sheet extent and flow on the continental shelf. The Antarctic Peninsula Ice Sheet (APIS) is now recognised to have terminated at the shelf edge at the Last Glacial Maximum (LGM), with ice streams occupying most of the cross-shelf bathymetric troughs (e.g., Pudsey et al., 1994; Larer and Vanneste, 1995; Canals et al., 2000, 2003; Ó Cofaigh et al., 2002; Evans et al., 2004; Heroy and Anderson, 2005, 2007; Anderson and Oakes-Fretwell, 2008). Advances in cosmogenic nuclide surface exposure dating of glacially-transported boulders and bedrock surfaces, optically stimulated luminescence (OSL) of beach cobbles, and radiocarbon dates of lacustrine and terrestrial deposits onshore constrain the timing of terrestrial ice retreat and especially ice-sheet thinning (e.g., Bentley et al., 2006, 2011; Johnson et al., 2011; Hodgson et al., 2013; Simkins et al., 2013; Glasser et al., 2014). Such palaeo-glaciological reconstructions have wider significance because they provide information on the former subglacial processes controlling ice sheet dynamics, for example, through imaging and sampling the former ice-sheet bed using ship-based geophysical methods and coring. Critically, they also provide observational constraints for testing and validating numerical ice-sheet models (e.g., King et al., 2012; Whitehouse et al., 2012a,b; Briggs and Tarasov, 2013). Finally, they provide a long-term palaeo-glaciological perspective on ice sheet change over centennial to millennial timescales.

There have been several syntheses of AP glacial history (Ingólfsson et al., 2003; Heroy and Anderson, 2005; Livingstone et al., 2012; Davies et al., 2012a). The aim of this paper is to summarise the current knowledge of the LGM to present ice sheet history for the AP and provide a series of time-slice reconstructions (isochrones in 5 ka steps) depicting changes in ice-sheet extent and thickness based on terrestrial and marine geomorphological and geological evidence. Tables of marine and terrestrial radiocarbon ages, terrestrial cosmogenic nuclide (TCN), optically stimulated luminescence (OSL), and relative palaeomagnetic intensity (RPI) ages are presented in the [Supplementary Information](#).

2. Study area

Physiographically, the AP consists of a thin spine of mountains that for much of its length forms a plateau 1800–2000 m in elevation, although exceptionally peaks can reach up to 3500 m asl.

The peninsula is fringed by a series of islands including, for the purpose of this review, the South Shetland Islands to the northwest (Fig. 1). The continental shelf surrounding the AP is incised by a series of cross-shelf bathymetric troughs with water depths that range from 500 m to more than 1000 m. The mountainous spine of the AP provides an orographic barrier to precipitation and, as a result the eastern AP has a polar continental climate further cooled by the large areas of ice shelves to the east and south and the clockwise flowing Weddell Gyre. By contrast, the western AP is subject to rates of snow accumulation of up to $1400 \text{ kg m}^{-2} \text{ yr}^{-1}$ (Thomas et al., 2008) delivered by the prevailing westerlies (Domack et al., 2003). On the western AP high precipitation results in high accumulation rates and low equilibrium line altitudes. In contrast, the eastern AP is colder with lower precipitation and as a result equilibrium line altitudes are higher and accumulation rates are lower.

Contemporary ice cover on the AP averages 500 m in thickness and covers about 80% of the landmass with a sea-level rise equivalent of about 242 mm (Pritchard and Vaughan, 2007), and an estimated contribution to eustatic sea level since the LGM of about 2.9 m (Heroy and Anderson, 2005). Ice drains eastwards and westwards towards the coast of the peninsula, with the majority of flow occurring as a series of outlet glaciers. The Larsen Ice Shelf occupies a large part of the eastern margin of the peninsula south of about 66° S . There are also smaller ice shelves on the southwestern AP around Alexander Island (Fig. 1). A number of these ice shelves have experienced recent dramatic retreat (e.g., Vaughan and Doake, 1996; Scambos et al., 2003; Holt et al., 2013).

3. Methods

This review includes a large database of marine and terrestrial radiocarbon, cosmogenic nuclide, optically stimulated luminescence and relative palaeomagnetic intensity (RPI) dates which can be used as minimum ages to constrain past ice sheet limits (Fig. 2; [Supplementary Data Table 1](#)). The database is an updated version of two recently published reviews (Livingstone et al., 2012; Davies et al., 2012a). Each age has a Map ID number, shown on Fig. 2, which can be cross referenced with the Map ID's given in the [Supplementary Information](#).

3.1. Marine geophysical records of ice-sheet extent

Evidence of former grounded ice on the AP continental shelf has been recorded by echo-sounding, acoustic sub-bottom profiler and seismic reflection data on multiple research cruises spanning many decades. With the advent of multibeam swath bathymetry it has been possible to identify and map glacial landforms, such as mega-scale glacial lineations (MSGLs), drumlins, meltwater channels and grounding-zone wedges (GZWs) in great detail (Fig. 3). This has facilitated comprehensive reconstructions of grounding-line limits during the LGM and subsequent deglaciation, and has permitted the identification of palaeo-ice stream troughs on the shelf (e.g., Livingstone et al., 2012).

Acoustic sub-bottom profiler data, using systems that transmit signals in the 1.5–5 kHz range, provide information about the physical nature of the upper few metres to several tens of metres of

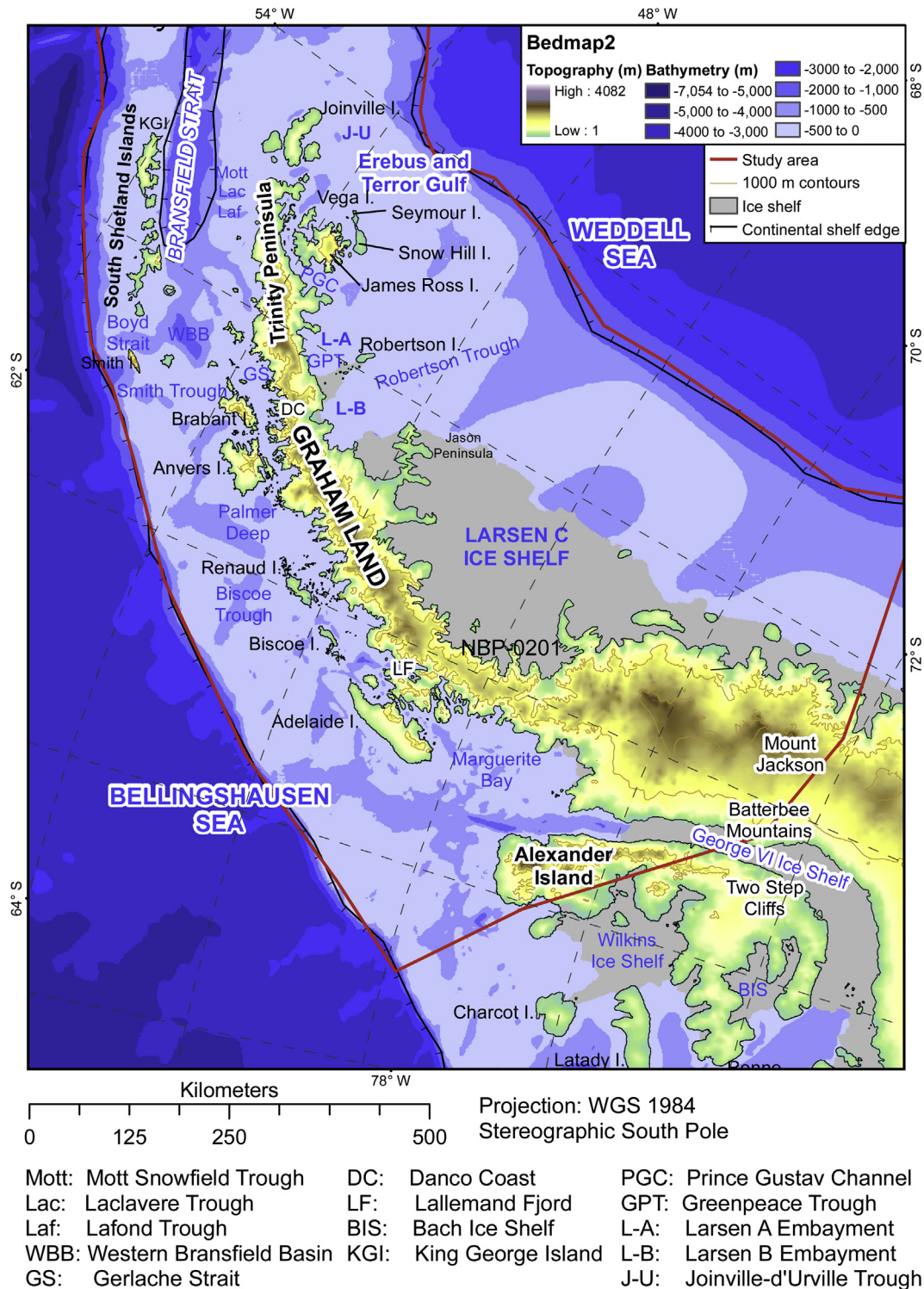


Fig. 1. The Antarctic Peninsula, showing the location of place-names referred to in the text. Current ice surface topography and bathymetry are shown, and are derived from the BEDMAP2 database (Fretwell et al., 2013). Modified from Davies et al. (2012a).

sea-floor sediments. This is helpful for selecting the locations of core sites and for the interpretation of geomorphological features and sedimentary structures related to glaciation. Seismic reflection profiles, using airgun and water gun sources, collected on the continental shelf during several research cruises, provide deep penetration of the seafloor sediments and solid geology (e.g. Larter

and Barker, 1989; Banfield and Anderson, 1995; Bart and Anderson, 1995; Larter et al., 1997; Smith and Anderson, 2010). This allows information to be collected on the bedrock geology and structure, as well as long-term patterns of sediment erosion and deposition, and the thickness and internal architecture of deeper sedimentary units.

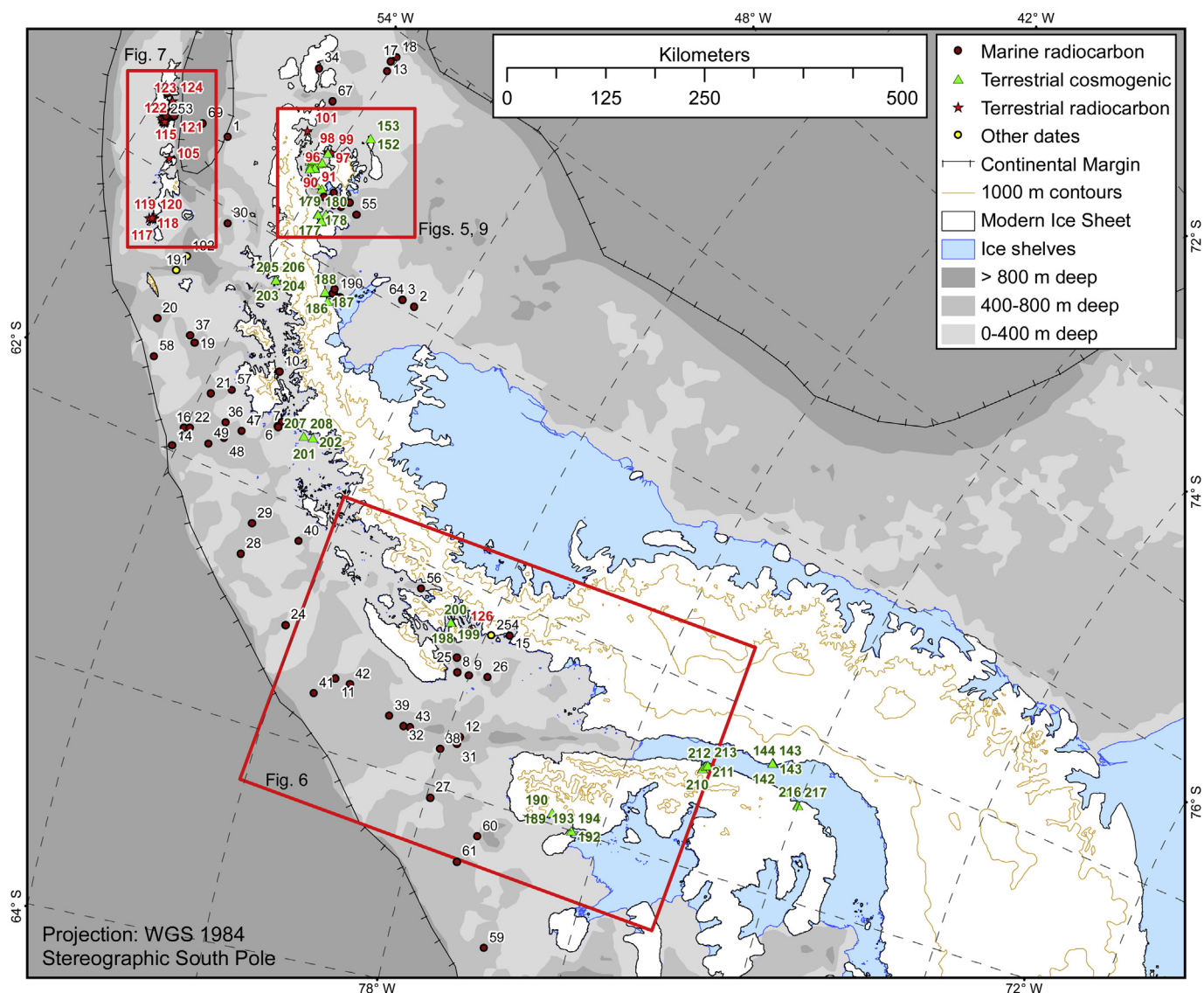


Fig. 2. Marine and terrestrial radiocarbon and terrestrial cosmogenic ages around the Antarctic Peninsula numbered according to Map ID. Please cross reference to [Supplementary Information Table 1](#). Inset boxes show the locations of [Figs. 5–7 and 9](#).

3.2. Continental shelf sediments

Sediment cores have been collected from the AP shelf using a range of coring devices including gravity-, piston-, kasten-, box- and vibro-corers as well as drill cores (Ocean Drilling Program Leg 178, SHALDRIL). [Supplementary Data Table 1](#) lists all the cores collected on the continental shelf from which radiocarbon dates have been obtained. The typical complete stratigraphic succession in these cores comprises a tripartite sequence of subglacial, proximal glaci-marine and open marine facies (e.g. Evans and Pudsey, 2002; Heroy and Anderson, 2007). Subglacial facies include a lower stiff, massive, matrix-supported diamicton (Dowdeswell et al., 2004a; Evans et al., 2005), which is a 'hybrid' lodgement-deformation till (Ó Cofaigh et al., 2005, 2007; Reinardy et al., 2011a,b); and an overlying soft, porous, massive, matrix-supported diamicton variously interpreted as either a subglacial deformation till or a hybrid deformation-lodgement till (e.g. Dowdeswell et al., 2004a; Evans et al., 2005; Ó Cofaigh et al., 2005, 2007; Heroy and Anderson, 2007; Reinardy et al., 2009, 2011a,b). On the eastern AP shelf and in Marguerite Trough the till is

frequently overlain by a transitional glaci-marine unit (defined here as grounding-line proximal glaci-marine sediments), which is often characterised by sub-parallel stratification, high pebble abundance and rare microfossils. Several authors have assigned the deposition of this unit to a sub-ice shelf setting (Evans and Pudsey, 2002; Brachfeld et al., 2003; Domack et al., 2005; Evans et al., 2005; Kilfeather et al., 2011). Other cores from Marguerite Trough and from within Marguerite Bay sampled a terrigenous mud unit that is virtually devoid of ice-rafted debris and biogenic material resting on proximal glaci-marine sediments. This unit was also interpreted as having been deposited in a sub-ice shelf environment (Kennedy and Anderson, 1989; Pope and Anderson, 1992; Kilfeather et al., 2011). The uppermost sediment facies on the AP shelf varies between bioturbated to laminated, diatom-bearing to diatomaceous silts and clays with rare dropstones that occur within the deeper troughs (e.g. Evans and Pudsey, 2002; Domack et al., 2005; Ó Cofaigh et al., 2005; Heroy and Anderson, 2007), and sand-rich (residual) glaci-marine sediments that occur on the shallower areas of the shelf and reflect the influence of strong marine currents (Pope and Anderson, 1992; Pudsey et al., 2001). Both of these

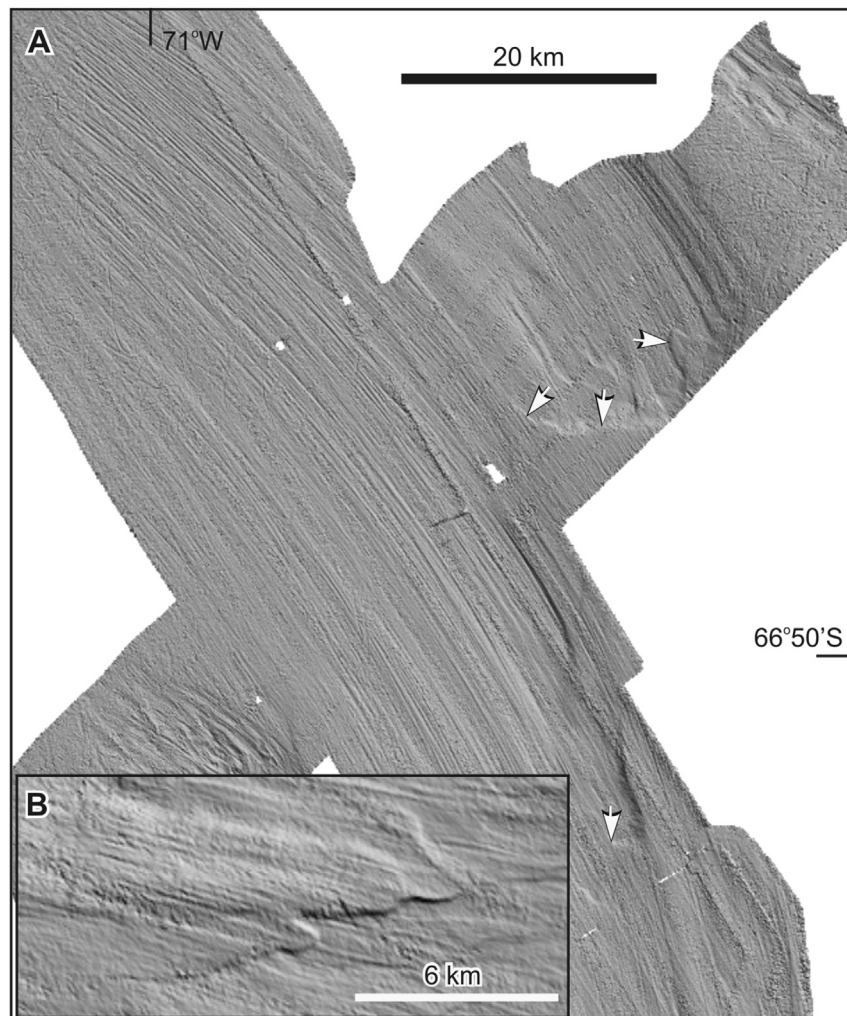


Fig. 3. (A) Shaded-relief image of swath-bathymetric data (grid-cell size 50 m × 50 m) showing mega-scale glacial lineations formed in sediment in outer Marguerite Trough (modified from Ó Cofaigh et al., 2005). Two localised occurrences of grounding-zone wedges on top of the lineations are arrowed. (B) Shaded relief swath bathymetry image of grounding-zone wedge (GZW), inner Larsen-A shelf (modified from Evans et al., 2005). Grid cell size 50 m × 50 m.

sediment facies reflect deposition in an open marine setting. This complete stratigraphic succession has been widely interpreted to record the advance and retreat of grounded ice across the AP shelf. Locally, variations may occur due to disturbance, such as where iceberg keels have furrowed the bed, or where fine-grained deposits have been winnowed to produce a lag.

3.3. Marine core chronology including problems and corrections

Ages constraining the retreat of grounded ice from the AP continental shelf following the LGM were compiled from published sources (Fig. 2; Supplementary Data Table 1). The majority of marine ages around the AP are from radiocarbon dating, although RPI dating techniques have also been used (cf. Brachfeld et al., 2003; Willmott et al., 2006).

For marine radiocarbon ages, we have assumed a uniform marine reservoir age of 1230 years (Domack et al., 2001; Brachfeld et al., 2002; Reimer et al., 2004a; Heroy and Anderson, 2007). Consequently, we corrected conventional radiocarbon dates on calcareous (micro-) fossils by subtracting the marine reservoir effect. In cases where the uncorrected radiocarbon ages were younger than 1230 years, the fossils were assumed to be of modern age (Domack et al., 2005; Milliken et al., 2009). We note, however,

that it is possible that the marine reservoir effect could have been much larger during the LGM (Sikes et al., 2000; Van Beek et al., 2002; Vandergoes et al., 2013). Hall et al. (2010a) argued that the Southern Ocean marine reservoir has been constant, at least for the last 6000 years, and recommend a slightly younger reservoir age of 1144 years. However, because surface sediment reservoir ages have been shown to vary widely, and to compare easily with the deglacial ages in other sectors of Antarctica, we apply a uniform correction for carbonates but apply local reservoir corrections for samples comprising the acid-insoluble fraction of organic material (AIO) (see below).

Radiocarbon ages were all calibrated with the Calib 6.0.2 programme, using the Marine09.14c curve for marine ages (Stuiver and Reimer, 1993; Reimer et al., 2004b, 2009). The ΔR value used in calibration (830) represents the difference between the “global” surface ocean ^{14}C age (400 years) and the regional surface ocean ^{14}C age (1230 ± 100 years) (Hughen et al., 2004; Hall et al., 2010a). All ages are reported as calibrated, in thousands of years before present (cal ka BP), where ‘present’ is AD 1950, and the two-sigma error range for each age is also given. The final age is rounded to the nearest decade. For the purposes of this publication, only ages associated with deglaciation (i.e., the minimum age for grounded ice-sheet retreat) are calibrated. Other down-core ages are

provided to aid the individual assessment of reliability (i.e., stratigraphic consistency, evidence for age reversals).

There are a number of possible errors in using marine radiocarbon dates obtained from organic matter to provide a minimum age for the retreat of grounded ice (cf. Andrews et al., 1999; Anderson et al., 2002; Heroy and Anderson, 2007; Hillenbrand et al., 2010b, 2013). In particular, because of the scarcity of calcareous microfossils in Antarctic shelf sediments, ^{14}C dates are frequently derived from AIO. However, even this material is often contaminated by large and unknown amounts of recycled, fossil organic carbon, which can yield older than expected dates. To account for this contamination effect, we applied a core-site specific correction by subtracting the AIO age of the undisturbed seafloor surface sediment recovered with a box corer from the down-core AIO ages of the corresponding vibro-, piston- or gravity core. At sites where no additional box core was recovered or no seabed surface sediment was dated, we used either a marine reservoir correction obtained from a nearby box core site or the core-top AIO age from the corresponding vibro-, piston- or gravity core itself for down-core age correction. This approach, however, assumes that the degree of contamination with fossil carbon and the ^{14}C age of the contaminating carbon have remained constant through time, which is rarely the case. For instance, a 'dog-leg' in age depth plots for sediment cores is often observed, resulting in a large down-core increase in the ^{14}C age of the deglacial unit (e.g. Domack et al., 1999; Pudsey et al., 2006; Heroy and Anderson, 2007; McKay et al., 2008; Smith et al., 2011). This is because the deglacial sediments at the base of the transitional unit are dominated by terrigenous components and therefore only contain a small amount of organic matter, whereas the supply of fossil carbon is likely to be higher because the ice-sheet grounding-line from which the contaminated carbon originated was located closer to the core site (cf. Domack, 1992). Given the above problems, we consider AIO ages to be less reliable than those derived from carbonate shells and microfossils. Radiocarbon ages from calcareous foraminifera can be considered particularly reliable, because delicate foraminifera tests are easily crushed and do not easily survive reworking.

To obtain a precise minimum age on the retreat of grounded ice, ideally the calcareous fossils within transitional glacial marine sediments lying directly above the subglacial till should be dated. Where this is not possible, overlying postglacial glacial marine muds or diatom-rich sediments can help constrain the onset of open-marine conditions, which in turn provides a minimum age for grounding-line retreat (Heroy and Anderson, 2007; Hillenbrand et al., 2010b; Smith et al., 2011). However, it should be noted that in some cases dates from this open marine facies can be significantly younger than the timing of initial retreat.

As described above, the reliability of deglaciation ages from marine sediment cores varies considerably with dating technique (AIO vs. carbonate radiocarbon ages), stratigraphic sequence and sediment facies (e.g., dates on iceberg turbate facies or cores that do not penetrate to the subglacial till are less reliable). To account for this we have devised a reliability index (from 1 to 3) (Supplementary Data Table 1) to distinguish between ages we are confident in from those that are deemed less reliable as minimum age constraints on deglaciation. The most reliable ages (score: 1) are radiocarbon ages on calcareous micro-fossils found in the transitional glacial marine unit. Moreover, the down-core ages must be in order, the core-top age (if available) must be close to the Southern Ocean marine reservoir age and there must be no evidence of bioturbation, iceberg turbation, or other sediment reworking as revealed by swath bathymetry data or sedimentary structures in the cores. We also assigned score 1 to a study that constrained the timing of grounded ice-sheet retreat from the eastern AP shelf by RPI dating (Brachfeld et al., 2003). Radiocarbon

dates are deemed less reliable (score: 3) if they were derived from AIO material, yielded a very old core-top age, were obtained from sedimentary sequences with down-core age-reversals or if subglacial till was not recovered at the corresponding core site. Unreliable deglaciation ages are also indicated by iceberg turbation (as revealed by iceberg scouring observed near a core site in swath bathymetry data or by an iceberg turbate facies detected in the core lithology) and/or evidence of bioturbation in cores. However, even with old core tops, it is still possible to obtain reliable downcore AIO ages, especially when AIO-dating is combined with other dating techniques (e.g., Hillenbrand et al., 2010b) or where samples are chosen carefully (e.g., Hillenbrand et al., 2010a; Smith et al., 2011). Recently, a new method of compound-specific radiocarbon dating of organic matter, which was applied to sediments from the eastern AP shelf, has allowed a significant reduction of the contamination effect caused by the admixture of reworked fossil organic material (Rosenheim et al., 2008).

3.4. Terrestrial geomorphological reconstructions of ice sheet thickness and extent

Geomorphological reconstructions of ice-sheet thickness and extent rely on a sound understanding of glacial processes. Using detailed sedimentological analysis and, more recently, mapping from high-resolution remotely sensed images, it is possible to make inferences regarding former ice sheet extent, thickness and style of glaciation, including thermal regime (e.g., Clapperton and Sugden, 1982; Bentley et al., 2006; Hambrey and Glasser, 2012). When combined with chronological methods such as radiocarbon dating, OSL or cosmogenic nuclide dating, it becomes possible to reconstruct the thickness and extent of former ice masses on land through time. Cosmogenic nuclide dating of glacially transported boulders or bedrock surfaces (Fig. 4) provides information on the horizontal and vertical dimensions of ice sheets (e.g., Fink et al., 2006; Applegate et al., 2012), and can allow a sensitive reconstruction of ice-sheet thinning history (e.g., Stone et al., 2003; Bentley et al., 2006; Mackintosh et al., 2007; Johnson et al., 2011).

3.4.1. Surface exposure dating using cosmogenic nuclides

Surface exposure dating using cosmogenic nuclides has been employed widely in Antarctica (e.g., Stone et al., 2003; Bentley et al., 2006, 2011; Mackintosh et al., 2007; Johnson et al., 2008, 2011; Balco et al., 2013). This is due to a frequent dearth of terrestrial organic material for radiocarbon dating, and the arid and windy climate which results in a lack of snow cover and low prevalence of weathering processes (Balco, 2011). Our database contains 91 published cosmogenic ^{10}Be ages, 16 ^{26}Al ages, 4 ^3He ages and 11 ^{36}Cl ages from the AP sector. These ages are shown in Supplementary Data Table 2, with the data used to calculate the ^{10}Be and ^{26}Al ages also included in Supplementary Data Table 3.

All ^{10}Be and ^{26}Al concentrations reported are blank-corrected. We have recalculated the published ^{10}Be and ^{26}Al ages in order to make them comparable. This was achieved by using the published information on each sample to recalculate the ages using version 2.2 of the CRONUS-Earth online exposure age calculator (Balco et al., 2008), and the most commonly-used scaling scheme, 'St' (Lal, 1991; Stone, 2000). We did not apply a geomagnetic correction. The uncertainties on the reported ages are all external, to enable comparison between sites many hundreds of kilometres apart. We applied the erosion rate that the original authors assumed (zero in all cases), a quartz density of 2.7 g cm^{-3} for each sample, and used the Antarctic pressure flag ('ant') for the input file. We took ^{10}Be and ^{26}Al concentrations, sample thicknesses, and shielding corrections from the original papers. The ^{10}Be and ^{26}Al concentrations for the 'BAT' samples were recalculated as described in Bentley et al.

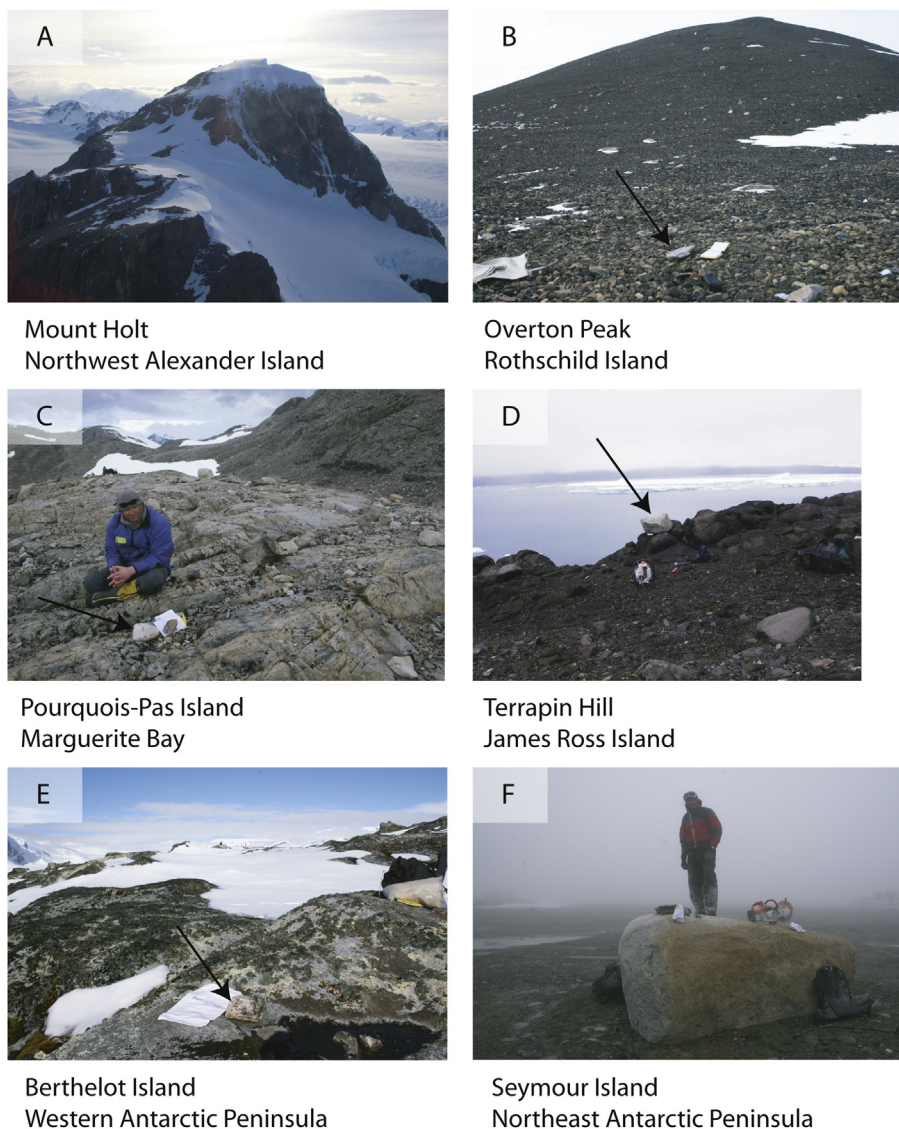


Fig. 4. Field photographs showing Antarctic Peninsula sites from which erratic and bedrock samples have been collected for cosmogenic dating. Small arrows indicate the position of the samples. References for the studies associated with each photograph are: A. [Johnson et al. \(2012\)](#); photograph by Jeremy Everest. B. [Johnson et al. \(2012\)](#); photograph by Phil Leat. C. [Bentley et al. \(2011\)](#); photograph by Mike Bentley. D. [Johnson et al. \(2011\)](#); photograph by Mike Bentley. E. [Bentley et al. \(2011\)](#); photograph by Mike Bentley. F. [Johnson et al. \(2012\)](#); photograph by Steve Roberts.

(2011), i.e. the original ETH-reported isotopic concentrations were reduced by 9.6% and 7.2% for ^{10}Be and ^{26}Al , respectively. The resulting concentrations were then used to calculate exposure ages with the CRONUS-Earth online calculator, using the 07KNSTD (^{10}Be) and KNSTD (^{26}Al) standardisations.

3.4.2. Terrestrial data from lakes, raised beaches and moss banks

Most terrestrial studies on the AP are limited to James Ross Island, Marguerite Bay and the South Shetland Islands. Lakes, raised beaches, moss banks and other terrestrial deposits can provide minimum ages for deglaciation and ice sheet fluctuations and also rates of postglacial isostatic uplift where they are at or below the Holocene marine limit. Organic matter is sparse in Antarctica, but microfossils within terrestrial lakes allow radiocarbon dating of the initiation of deposition, indicating deglaciation, and the transition from marine to freshwater conditions, indicating isostatic uplift above regional sea level ([Roberts et al., 2009, 2011](#); [Watcham et al., 2011](#)). Lake sediments can also provide a sensitive record of modern

and Holocene environmental conditions and climate (e.g. [Björck et al., 1996a, 1996b](#); [Smith et al., 2006](#); [Sterken et al., 2012](#); [Fernandez-Carazo et al., 2013](#); [Hodgson et al., 2013](#)). One of the main advantages of these records is the absence of a marine reservoir effect when freshwater macrofossils are dated. Terrestrial radiocarbon ages from lakes are reported in [Supplementary Data Table 4](#).

Other terrestrial deposits can also provide minimum ages for deglaciation and relative sea level change, for example raised beaches, such as those that are common on the South Shetland Islands (e.g. [Hall, 2010](#)), and the onset of accumulation of moss banks ([Björck et al., 1991b](#); [Royles et al., 2013](#)). Raised marine deposits can be dated using a combination of radiocarbon dating of shells, bones, and seaweed preserved within them ([Supplementary Data Table 4](#)) and OSL ([Supplementary Data Table 5](#)). Radiocarbon ages on marine animals require correction for the marine reservoir effect, which varies among different species groups (e.g. [Berkman et al., 1998](#); [Domack et al., 2005](#)).

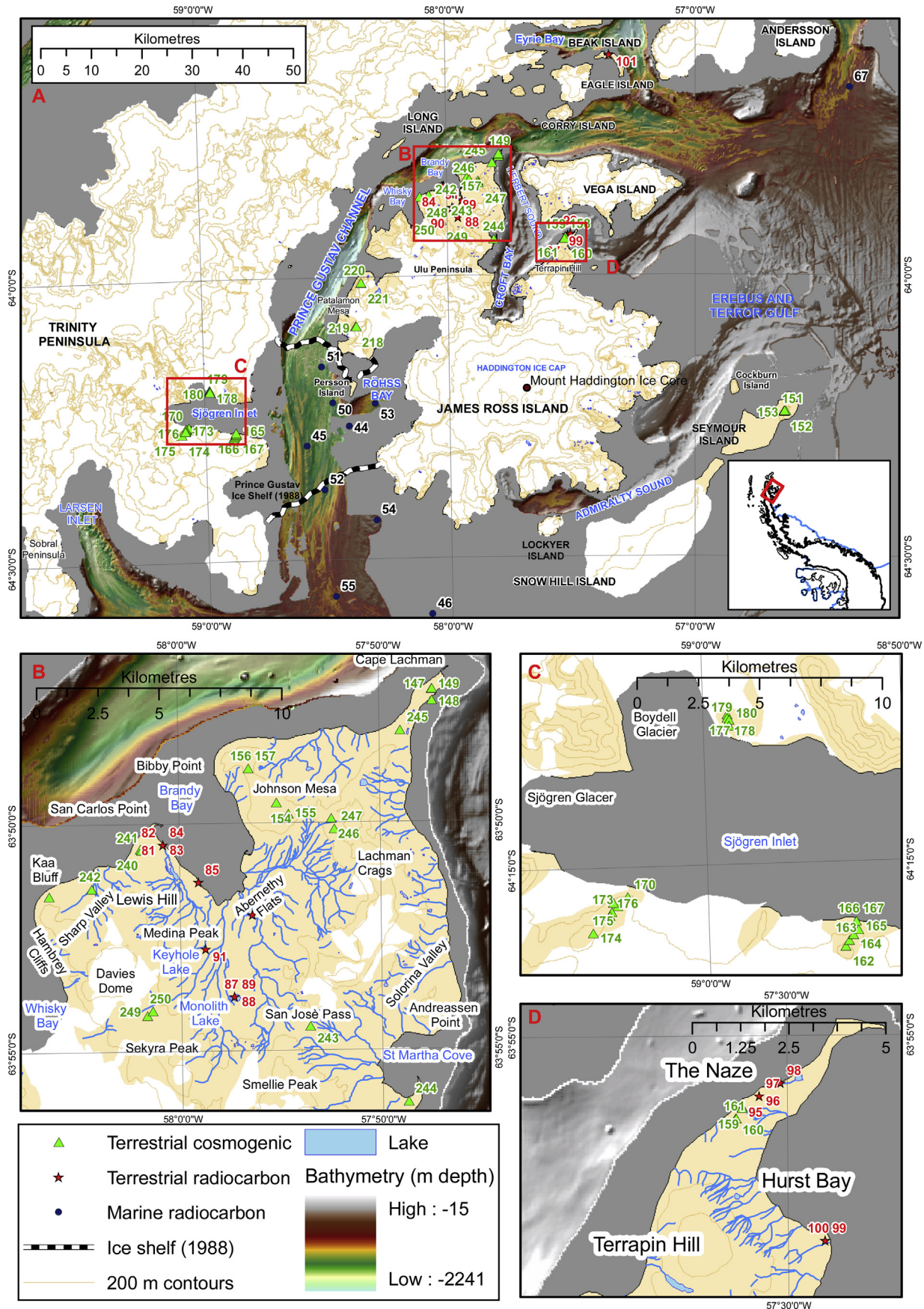


Fig. 5. (A) Marine and terrestrial radiocarbon and terrestrial cosmogenic ages around the northeast Antarctic Peninsula and James Ross Island numbered according to Map ID. Inset shows wider location. Red squares indicate location of larger-scale images. Please cross reference to [Supplementary Information tables](#). Location is shown on [Fig. 2](#). (B) Map IDs on Ulu Peninsula, James Ross Island. (C) Map IDs on Sjögren Inlet, Trinity Peninsula. (D) Map IDs on Terrapin Hill, James Ross Island.

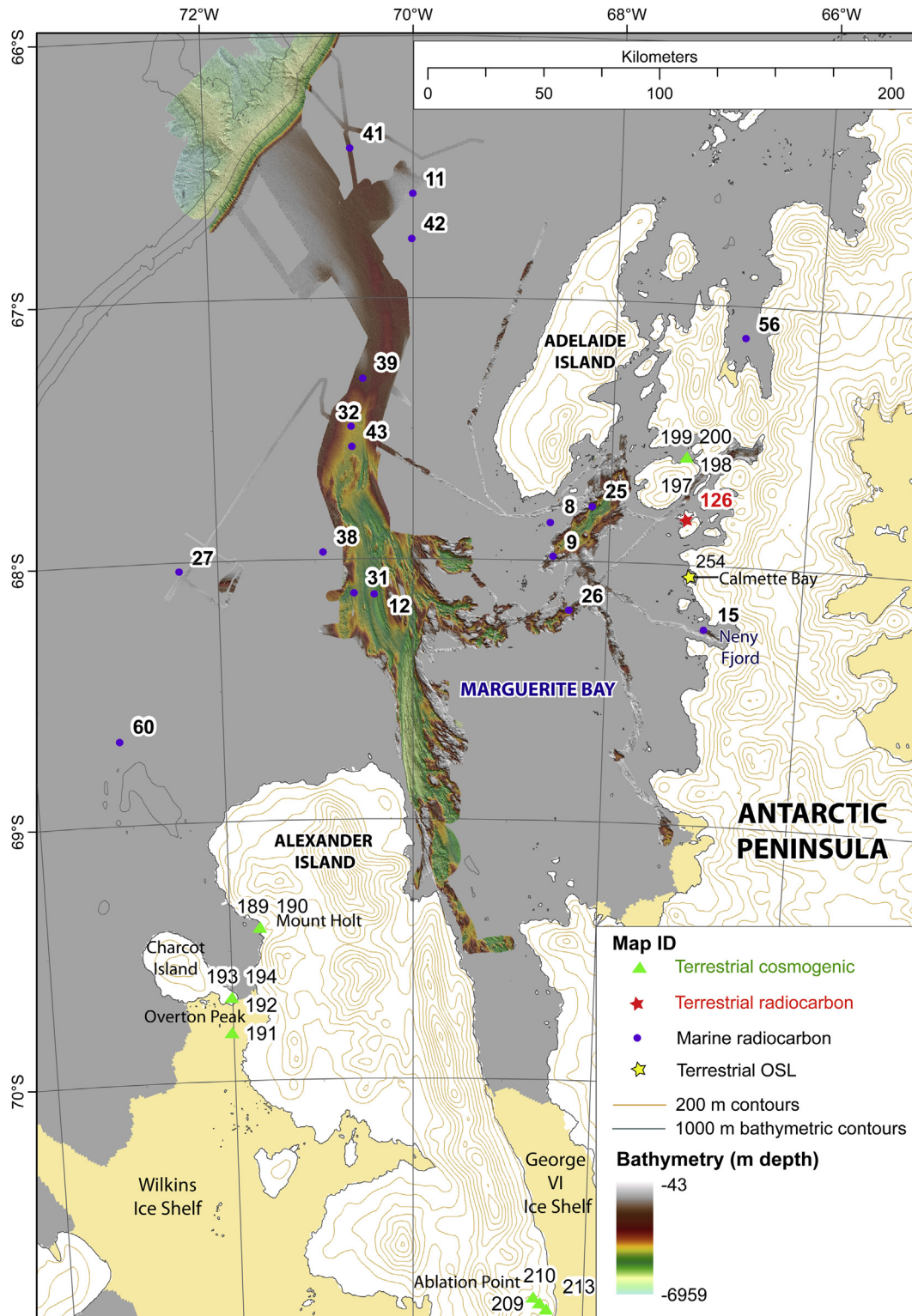
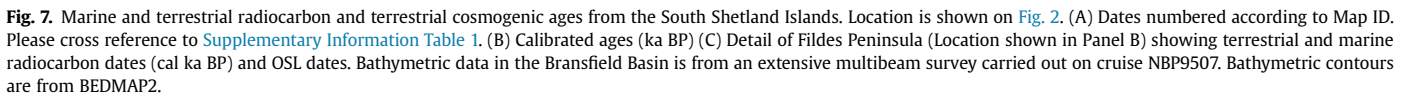


Fig. 6. Marine and terrestrial radiocarbon and terrestrial cosmogenic ages from Marguerite Bay numbered according to Map ID. Please cross reference to [Supplementary Information tables](#). Location is shown on [Fig. 2](#).

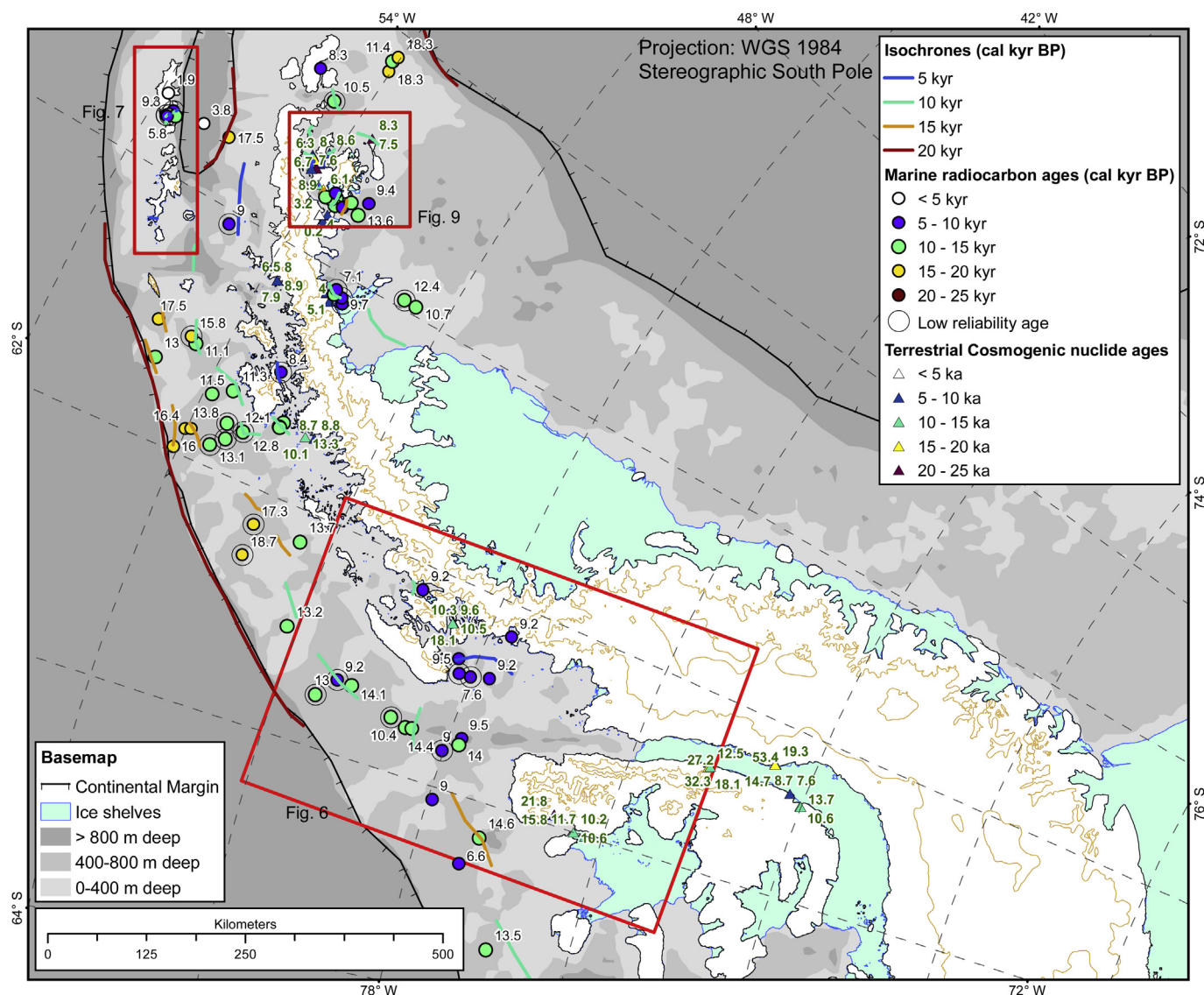
4. Ice sheet reconstruction – time slices

Reconstructions are shown at 5 ka intervals: 25 ka, 20 ka BP, 15 ka BP, 10 ka BP, 5 ka BP and 0 ka BP (Twentieth Century). [Figs. 2 and 5–7](#) show calibrated marine and terrestrial deglaciation ages

across the AP and South Shetland Islands and these data have been used to draw isochrones ([Figs. 8 and 9](#)). The locations with chronological constraints on ice-sheet retreat plotted in [Figs. 6 and 7](#) are predominantly sites of marine sediment cores, whose dates provide only *minimum* ages for deglaciation. This must be borne in mind



The terrestrial evidence for the configuration of the APIS at 25 ka BP is sparse. Most data come from northern James Ross Island and Marguerite Bay (Figs. 5 and 6). Granite erratics at elevations of up to 370 m asl on Ulu Peninsula, James Ross Island, indicate glacial overriding during the last glaciation (Davies et al., 2013; Glasser et al., 2014). The thickness of ice cover at 25 ka BP in this region



exceeded this altitude. Johnson et al. (2009) suggested from ³He surface exposure dating that James Ross Island was likely completely ice-covered at the LGM but that the ice cover was probably not much thicker than present. The Mount Haddington Ice Cap appears to have remained as a distinct ice dome that was confluent with the APIS at this time. This is based on isotopic evidence from the James Ross Island Ice Core which indicates that the ice there was not overrun by isotopically colder ice from the mainland (Mulvaney et al., 2012). Further south, near the Sjögren-Boydell and Drygalski Glaciers (Fig. 5C), cosmogenic dating suggested the ice sheet surface at 25 ka BP was thicker; locally at least 520 m above present sea level at the modern coastline (Map ID 162), with cold-based ice present at altitudes above 100–150 m asl (Balco et al., 2013).

In Marguerite Bay the first evidence of the onset of deglaciation is the colonisation of a lake on Horseshoe Island by eggs of the freshwater fairy shrimp *Branchinecta gaini*, which are present in the sediment matrix from 21.1 ka BP (Map ID 126; Fig. 6) (Hodgson et al., 2013). This indicates the existence of a perennial water body and requires at least one part of the ice sheet in inner Marguerite Bay to have been less than 140 m thick (relative to present sea level) at this

time. This event coincides with continued ice thinning in Moutonnée Valley (Bentley et al., 2006), and occurs shortly after the retreat of ice in the Bellingshausen Sea, which reached the mid-shelf by 23.6 cal ka BP (Hillenbrand et al., 2010a). On land, cosmogenic nuclide exposure ages from NW Alexander Island and Rothschild Island (Figs. 2 and 4) show progressive ice thinning since at least 22 ka BP, reaching an elevation of c. 440 m by 10.2–11.7 ka BP (Johnson et al., 2012). More widely, additional evidence of warming at this time comes from further north in the Scotia Sea where both the winter and summer sea-ice edges experienced a rapid melt-back event between 23.5 and 22.9 cal ka BP (Collins et al., 2012). Further south, in the western Amundsen Sea Embayment, deglaciation was probably underway as early as 22.3 cal ka BP (Smith et al., 2011). These events coincide with, or immediately post-date Antarctic Isotopic Maximum 2 (23.5 cal ka BP) seen in Antarctic ice cores (EPICA, 2006) and Southern Ocean sea surface temperature records (Kaiser et al., 2005).

On the South Shetland Islands at the LGM, grounded ice extended onto the outer continental shelf 50 km north of its present location, while on the southern side of the archipelago it extended seaward of the mouths of fjords and straits to the steep

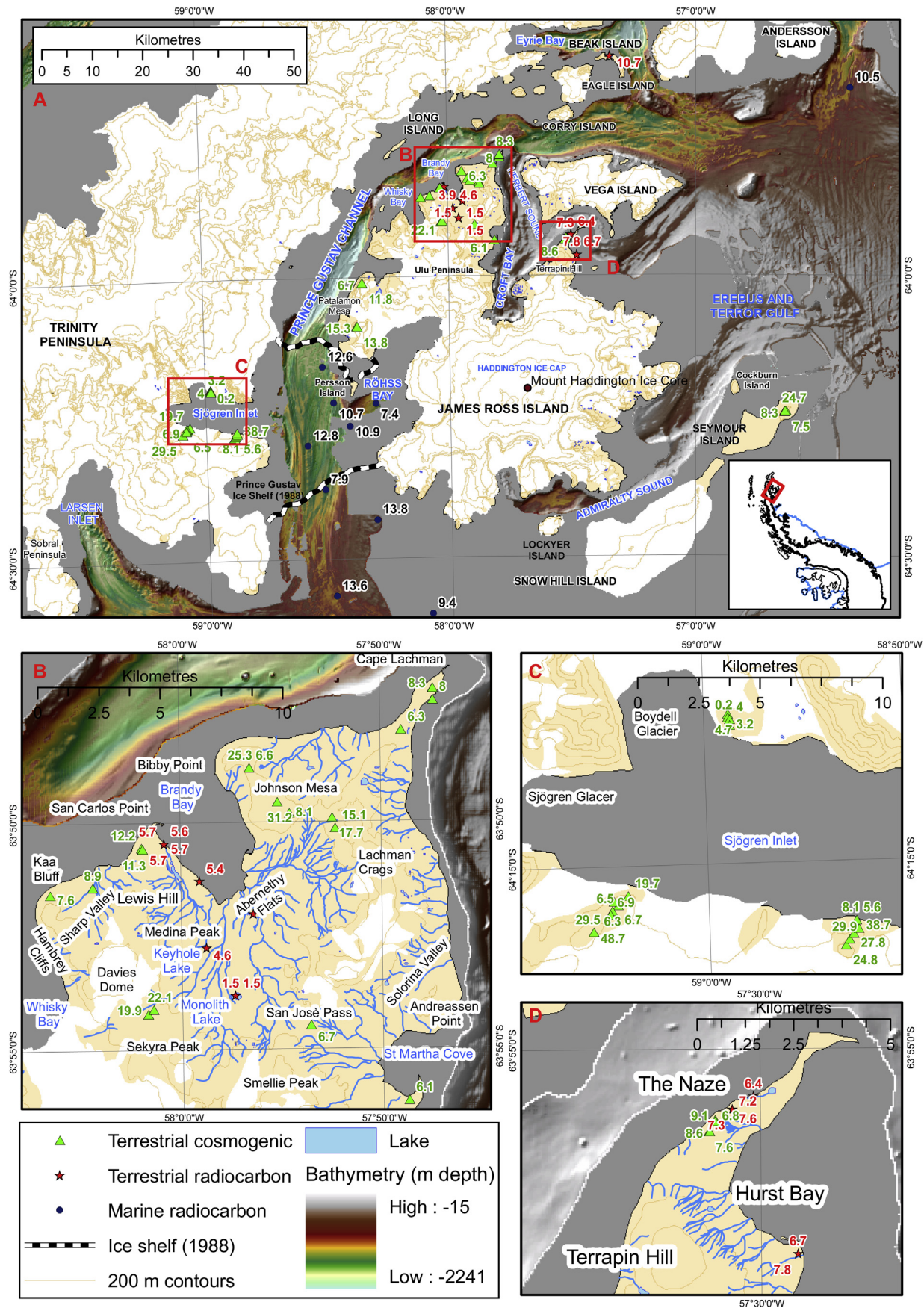


Fig. 9. (A) Marine and terrestrial ages around the northern Antarctic Peninsula and James Ross Island. Please cross-reference to Map IDs in Fig. 5. Location is shown on Fig. 2. Inset shows wider region. Location of larger scale maps is indicated by red squares (B–D). (B) Larger-scale map of Ulu Peninsula, James Ross Island. (C) Larger-scale map of Sjögren Inlet, Trinity Peninsula. (D) Larger-scale map of Terrapin Hill, James Ross Island.

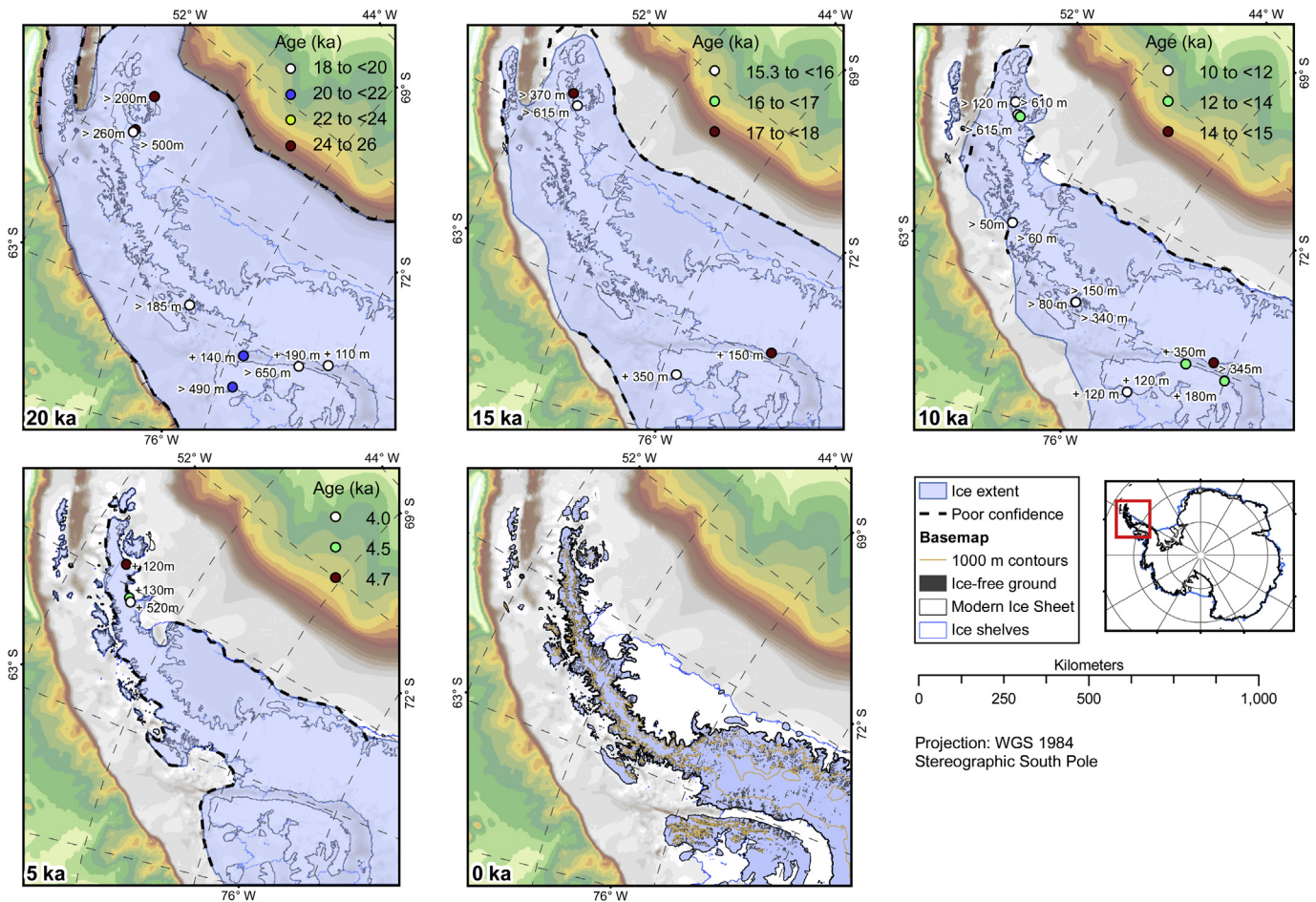


Fig. 10. Reconstructed time-slices for the Antarctic Peninsula Ice Sheet at 20, 15, 10, 5 and 0 ka. Note the ice sheet extent at 25 ka is regarded as the same as at 20 ka. Points on the maps indicate palaeo ice-sheet thickness (difference to present above present sea level [+ or –]), derived from cosmogenic nuclide ages. The current bed bathymetry is shown at 200 m intervals (derived from BEDMAP2; Fretwell et al., 2013). Minimum ice sheet thicknesses are indicated with a '>' sign.

northern boundary of Bransfield Basin (Figs. 7 and 10) (Simms et al., 2011). Sediment eroded from the fjords was deposited in a series of prominent submarine fans that extend into Bransfield Basin. Based on the present (estimated) water depth of the till/bedrock interface at the SHALDRIL core site in Maxwell Bay, Simms et al. (2011) concluded that the LGM ice cap must have been at least 570 m thick in the bathymetric troughs to be able to ground there. The South Shetland Islands do not appear to have been overridden by the APIS during the LGM, but rather were covered by an independent ice cap centred between Robert and Greenwich Islands (John and Sugden, 1971; Fretwell et al., 2010).

4.2. 20 ka BP

As with the 25 ka BP timeslice, there is a similar dearth of chronological data to constrain the ice sheet margin at 20 ka, and its position is largely based on the datasets outlined above (Fig. 10). Thus in the northern and north-eastern AP it is likely that the ice sheet margin remained grounded at or close to the shelf break in Vega and Robertson troughs from 25 to 20 ka BP. AMS ^{14}C ages from cores PC04 and PC06, which were recovered landward and seaward of a GZW offshore from Vega Trough, provide the only direct constraint for ice sheet retreat from the outer shelf (Heroy and Anderson, 2005, 2007). Radiocarbon ages on AIO- (PC04) and foraminifera (PC06) indicate that the APIS had retreated landward of the wedge by 18.3 cal ka BP (Figs. 2 and 8; Supplementary Data

Table 1, Map IDs 13 and 19). Only two other AIO ages (from sites VC266 and VC270 in the Larsen Inlet Trough) yielded calibrated ages of 16.7 and 17.4 cal yr BP, respectively (Pudsey et al., 2006). However, given the high contamination by fossil organic carbon in this area, particularly along the flow path of Larsen Inlet, we assign a low confidence to the reliability of these ages and do not include them in our time-slice reconstruction (Fig. 10). Finally granite boulders on the summit of Lachman Crags (370 m asl) became exposed on Ulu Peninsula, northern James Ross Island, at 17.7 ± 0.8 ka, while basalt boulders near Davies Dome at elevations of 312 m and 244 m yielded ages of 19.9 ± 7.3 and 22.1 ± 6.6 ka, indicating that ice-sheet thinning on James Ross Island followed initial recession of grounded ice from the continental shelf edge at ~ 20 ka (Glasser et al., 2014, Fig. 5B). Overall the retreat trajectory of grounded ice from its shelf edge position at 18.3 cal yr BP to the mid-inner shelf is poorly constrained.

On the western AP, seafloor geomorphological data, complemented by high-resolution seismic studies and sediment cores, reveal the pervasive extension of grounded ice to, or close to, the continental shelf edge at the LGM (e.g., Pope and Anderson, 1992; Pudsey et al., 1994; Larter and Vanneste, 1995; Banfield and Anderson, 1995; Ó Cofaigh et al., 2002; Evans et al., 2004; Heroy and Anderson, 2005; Ambblas et al., 2006; Graham and Smith, 2012). This includes prominent glacial unconformities that can be traced to the shelf break, streamlined subglacial landforms that extend uninterrupted across the shelf and subglacial till in cores.

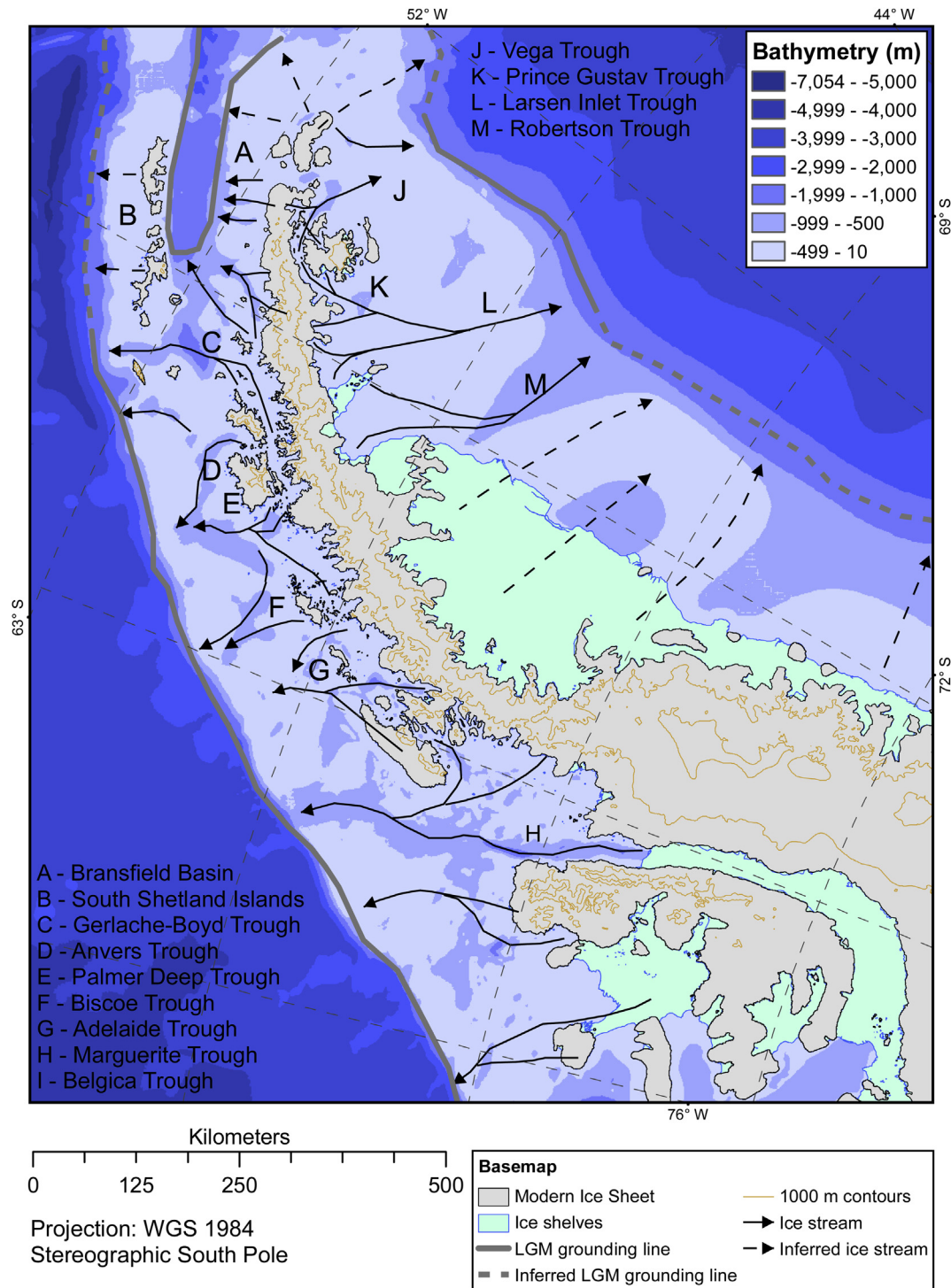


Fig. 11. Reconstruction of palaeo-ice stream drainage on the Antarctic Peninsula at and subsequent to, the LGM. Individual ice streams show a strong relationship to cross-shelf bathymetric troughs. Ice streams represented by dashed lines are tentative. Based on numerous reconstructions including: Bentley and Anderson, 1998; Canals et al., 2000, 2003; Camerlenghi et al., 2001; Ó Cofaigh et al., 2002, 2005; Willmott et al., 2003; Dowdeswell et al., 2004b; Evans et al., 2005; Heroy and Anderson, 2005, 2007; Ambilas et al., 2006; Bentley et al., 2006, 2010; Domack et al., 2006; Sugden et al., 2006; Graham and Smith, 2012; Livingstone et al., 2012; Davies et al., 2012a.

The identification of cross-shelf troughs with MSGLs, drumlins, grooved and streamlined bedrock and GZWs, provides evidence that flow was organised into ice-streams likely separated by slower moving ice on neighbouring banks (Fig. 11) (cf. Larter and Cunningham, 1993; Heroy and Anderson, 2005; Livingstone et al., 2012; Davies et al., 2012a). These ice streams are thought to have

been active at the LGM and throughout deglaciation. They include the Lafond, Laclavere, Mott Snowfield and Orleans palaeo-ice streams that drained into the Bransfield Basin; the Gerlache-Boyd, Biscoe, Adelaide, Anvers-Hugo, Smith and Marguerite Bay palaeo-ice streams that drained the western AP; and the Rothschild and Charcot palaeo-outlet glaciers (Fig. 11).

On the western AP shelf marine radiocarbon ages documenting the initial retreat of ice from the shelf edge reveal a general chronological pattern with recession progressing from north to south, with some variability (cf. Heroy and Anderson, 2007; Livingstone et al., 2012). A radiocarbon age of 17.5 ± 0.8 cal ka BP (carbonate material) obtained from transitional glacial marine deposits in core PC48 on the outer shelf of the Lafond Trough, east of Bransfield Basin (Figs. 2 and 8; Supplementary Data Table 1, Map ID 1), indicates grounding-line retreat from the shelf edge was underway prior to ~ 17.5 cal ka BP (Banfield and Anderson, 1995). Moraines imaged in seismic data on the outer shelf of Lafond and Laclavere troughs (Banfield and Anderson, 1995), landward of PC48, document a subsequent slow-down or pause in retreat. On the outer shelf of Smith Trough an age of 17.5 ± 1.09 cal ka BP (planktonic and benthic foraminifera), was obtained from transitional glacial marine deposits in core PC22 (Supplementary Data Table 1, Map ID 20) and indicates an equivalent timing of retreat (Heroy and Anderson, 2007). Although swath bathymetry data reveal streamlined glacial landforms in excess of 100 km in length on the outer-shelf of the Gerlache-Boyd Strait (Canals et al., 2000, 2002, 2003; Willmott et al., 2003), the initial timing of ice retreat back from the outer shelf in this location is unknown. This is due to the thick (up to ~ 60 m) drape of glacial marine sediment, which has made it difficult for cores to penetrate through to subglacial till (Heroy and Anderson, 2005).

On the outer-shelf of Anvers Trough ages of 16.4–15.4 cal ka BP constrain grounding-line retreat to before ~ 16.4 cal ka BP (Heroy and Anderson, 2007) (Figs. 8 and 10). Conversely, an age of 13.0 ± 0.59 cal ka BP (AIO material) taken from transitional glacial marine deposits in core GC03 (Map ID 58) on the bank between Anvers and Smith troughs, implies the shallower inter-ice stream bank may have remained glaciated for longer (Yoon et al., 2002). Lift-off of grounded ice in outer Orleans Trough must have occurred before 9.0 ± 0.7 cal ka BP (AIO material in core PC61; Map ID 30), but the corresponding date was obtained from transitional glacial marine deposits ~ 70 cm above the contact with subglacial till and it may therefore be considerably younger than the actual timing of initial retreat (see Heroy and Anderson, 2007). The oldest deglacial ages of 18.7 ± 0.46 cal ka BP (core PC55, Map ID 28) and 17.3 ± 0.8 cal ka BP (core PC57, Map ID 29) are ^{14}C dates on AIO from two cores collected on the outer shelf of Biscoe Trough (Figs. 2 and 8; Supplementary Data Table 1) which do not correspond to the north–south pattern of retreat. However, these ages are considered unreliable on account of their collection from sediment with very low total organic carbon content (Heroy and Anderson, 2007).

On northwest Alexander Island, cosmogenic nuclide ages indicate that during the LGM, the APIS was at least 490 m thicker than present, with thinning occurring from 21.8 ka (Figs. 2 and 6; Map ID 190) until 10.2 ka (Johnson et al., 2012). At Moutonnée Valley on eastern Alexander Island, exposure ages on boulders from nunataks and cols indicate that the LGM ice surface was at least 650 m thicker than at present, with thinning starting after 27.2 ka (Map ID 212; Fig. 8; Bentley et al., 2006). This agrees with similar exposure ages from the Batterbee Mountains, western Palmer Land, which indicate thinning to below 430 m asl by 17.7 ka (Map ID 141, Figs. 2 and 8; Supplementary Table 1) (Bentley et al., 2006).

4.3. 15 ka BP

By 15 cal ka BP ice in the most northerly troughs had retreated back from the shelf edge onto the outer or even the middle shelf (Bransfield Basin, Smith and Anvers troughs, and possibly Biscoe Trough) (Fig. 10). Ice may have remained grounded for longer on the shallower inter-ice stream banks in this northern zone (e.g. Yoon et al., 2002), while there is no evidence of retreat prior to 15 cal ka BP south of Biscoe Trough. The islands around the north-

eastern AP were probably still covered by ice around 15 cal ka BP (Fig. 10). The ice cap on James Ross Island was still confluent with the APIS (Johnson et al., 2011), although higher ground (above ~ 370 m) on Ulu Peninsula was ice-free (Glasser et al., 2014). Southwest Vega Island was deglaciated by 11.9 cal ka BP (Zale and Karlén, 1989) (Fig. 9).

Further south, retreat is thought to have begun around 15 ka BP as suggested by ages of 14.1 ± 1.0 cal ka BP (carbonate material) from transitional glacial marine facies on the outer shelf of Marguerite Bay (core PD88-85; Map ID 42) (Pope and Anderson, 1992), and 13.2 ± 0.65 cal ka BP (AIO material) from transitional glacial marine facies on the outer shelf of Biscoe Strait (core PC30; Map ID 24) (Heroy and Anderson, 2007) (Fig. 10). The onset of open marine conditions on the outer shelf part of Charcot Trough (core GC471, Map ID 59) and the mid-shelf of Rothschild Trough (core GC514, Map ID 60) is dated to 13.5 ± 0.48 cal ka BP and 14.5 ± 1.0 cal ka BP (both on AIO), respectively, providing minimum ages for retreat of grounded ice in this region (Graham and Smith, 2012) (Figs. 2 and 8; Supplementary Data Table 1).

Well-constrained chronologies enable detailed reconstructions for several troughs. In Marguerite Trough, radiocarbon ages on calcareous microfossils ranging from 14.4 to 14.0 cal ka BP (Fig. 6), suggest a period of rapid retreat across a ~ 140 km stretch of the outer shelf (Kilfeather et al., 2011), whilst a number of GZWs farther inland suggest that retreat became increasingly episodic (Jamieson et al., 2012; Livingstone et al., 2013). Radiocarbon ages of 13.8–11.1 cal ka BP obtained from biogenic carbonate and AIO document rapid retreat of the Anvers Trough palaeo-ice stream into Palmer Deep on the inner shelf (see Pudsey et al., 1994; Domack et al., 2006; Livingstone et al., 2012) (Figs. 2, 8 and 10).

Cores from the mouth of Prince Gustav Channel suggest that the transition from grounded to floating ice commenced at 13.6 cal ka BP (Map ID 55), and that the grounding-line reached the Röhss Bay area between 10.9 and 10.7 cal ka BP (Fig. 9) (Pudsey and Evans, 2001; Evans et al., 2005; Pudsey et al., 2006). It is also possible that grounded ice retreated south–north and north–south along Prince Gustav Channel, with a date obtained from core VC238 indicating that grounded ice had retreated to a position NW of Persson Island by 12.6 cal ka BP (Map ID 51, Figs. 5 and 9). Cosmogenic nuclide ages on granite boulders associated with moraine fragments and granite-rich drifts at ~ 100 m asl on western Ulu Peninsula next to Prince Gustav Channel, indicate evacuation of the ice stream from the northern part of the channel by ~ 12 ka (Fig. 9) (Glasser et al., 2014). This coincided with a period of peak warmth recorded in the Mount Haddington ice core (Mulvaney et al., 2012). Samples from the Batterbee Mountains yielded a range of ages, possibly suggesting complex exposure histories (Bentley et al., 2006, 2011). The youngest age from the plateau (12.7 ka; 350 m asl) is assumed to be the most representative of the timing of the last deglaciation of these mountains (Bentley et al., 2006).

On the South Shetland Islands, a long SHALDRIL core, as well as other cores and seismic data, constrain the timing and spatial extent of glacial retreat within Maxwell Bay, on the south side of King George Island. The oldest date from shell fragments in glacial marine sediments in the SHALDRIL core is 13.7 cal ka BP (Map ID 76, Fig. 7; Supplementary Data Table 1), with extrapolation of the age model suggesting that grounded ice decoupled from the bed in Maxwell Bay at 14.8–14.1 cal ka BP (Milliken et al., 2009; Simms et al., 2011). This age predates minimum deglaciation ages based on AIO dates from Maxwell Bay (Li et al., 2000) and eastern Bransfield Basin (Heroy et al., 2008) by 4–5 ka, but it is consistent with terrestrial evidence from Barton Peninsula, King George Island, where Seong et al. (2009) published a maximum age of deglaciation of 15.5 ± 2.5 ka from cosmogenic nuclide dating of

glacial surfaces (Map ID 224; [Supplementary Data Table 2](#)). Following the onset of deglaciation, ice retreated 15–20 km to a mid-fjord pinning point and stabilised until ca 10.1 cal ka BP, after which there was a transition from perennial floating ice to open marine conditions in Maxwell Bay and Bransfield Basin ([Simms et al., 2011](#)).

4.4. 10 ka BP

Along much of the eastern AP margin grounded ice is likely to have approached its present configuration by ~10 cal ka BP, with fringing ice shelves at, or bigger than, 20th century pre-collapse limits. North of Prince Gustav Channel, core KC49 provides a minimum age for deglaciation of Erebus and Terror Gulf at 10.5 cal ka BP (Map ID 67; [Figs. 5 and 9](#)) based on ramped-pyrolysis ^{14}C dating ([Rosenheim et al., 2008](#)). The transition from grounded ice to floating ice in the Larsen-A and Larsen-B embayments is well-constrained by RPI and ^{14}C dating of foraminifera and AIO; the ages from both techniques are remarkably consistent, with the transition occurring at 10.7–10.6 cal ka BP ([Figs. 2 and 8](#); [Supplementary Data Table 1](#)) ([Brachfeld et al., 2003](#); [Domack et al., 2005](#)). AIO ^{14}C dates from Larsen Inlet and Robertson Trough show greater scatter probably associated with a higher degree of contamination from fossil carbon, whereas AIO ages from the southern mouth of Prince Gustav Channel indicate a slightly earlier recession of grounded ice (13.6–13.8 cal ka BP; [Pudsey et al., 2006](#)). [Evans et al. \(2005\)](#) suggested that initial deglaciation of troughs in these areas was continuous (and possibly rapid) on account of the absence of recessional features. In contrast, GZWs across the shelf of the northern Larsen-A sector and south of Prince Gustav Channel ([Fig. 5](#)) indicate that ice retreat in the region was punctuated by stillstands ([Evans et al., 2005](#); [Reinardy et al., 2011b](#)). However, neither the rapidity nor evidence for stillstands is resolved by the available ^{14}C dates. By 10 ka, ice in Prince Gustav Channel, and the Larsen-A and Larsen-B sectors had receded to near modern limits. The ice sheet was at least 300–500 m thicker than present prior to 9 ka ([Fig. 10](#)) ([Balco et al., 2013](#)).

Approximately 40 km north of James Ross Island, dates on marine sediments from an isolation basin on Beak Island suggest that it was ice-free by 10.7 ± 0.68 cal ka BP (Map ID 101; [Figs. 2 and 9](#)) ([Roberts et al., 2011](#); [Sterken et al., 2012](#)). At present, only limited marine geological ([Curry and Pudsey, 2007](#)) and no chronological data are available from south of Jason Peninsula so the configuration and timing of deglaciation of this sector of the APIS remains unknown.

Grounded ice retreated from the protected inner shelf and fjord environments along the AP coast during the early Holocene. Core PD-91/PC-08 constrains deglaciation of Croft Bay/Herbert Sound to 8.4 cal ka BP ([Figs. 5 and 9](#)) ([Minzoni et al., 2011](#)). This is consistent with the high-resolution climate record from Firth of Tay 100 km further to the north, which constrains grounded ice retreat to before 8.3 cal ka BP and probably at 9.4 cal ka BP (Map ID 34) ([Michalchuk et al., 2009](#)).

On the western AP continental shelf, the 10 ka time-slice documents grounded ice on the inner shelf of most regions, with the exception of Marguerite Trough where [Kilfeather et al. \(2011\)](#) suggested that ice was still grounded on the mid-shelf ([Fig. 10](#)). This reconstruction is based on an age of 9.5 ± 0.6 cal ka BP, taken from a shell in the transitional glaciomarine unit of a core from the mid-shelf of Marguerite Trough (Map ID 12; [Figs. 2 and 8](#)), and corroborated by an age of 9.0 ± 1.18 cal ka BP derived from a shell in transitional glaciomarine deposits recovered from a subsidiary trough just to the southwest (Map ID 27) ([Heroy and Anderson, 2007](#)). These ages may, however, be much younger than the actual timing of the retreat of grounded ice. Retreat back across the

inner-shelf of Marguerite Bay must then have been rapid as indicated by the onset of diatomaceous sedimentation, indicative of seasonally open marine conditions in Neny Fjord on the inner shelf of Marguerite Bay by 9.2 ± 0.6 cal ka BP (core JPC43; Map ID 15) ([Allen et al., 2010](#)).

Thinning and rapid ice recession in Marguerite Bay around this time is also supported by terrestrial evidence. At Horseshoe Island, aquatic mosses were present in lakes at c. 80 m above present sea level from 10.6 ± 0.1 cal ka BP, although dates on bulk organic material from the lake suggest the onset of deglaciation at the site as early as 28–22.5 cal ka BP ([Hodgson et al., 2013](#); Map ID 126; [Fig. 2](#)). Surface exposure dates at Parvenu Point on Pourquois-Pas Island (283 m asl) indicate rapid early Holocene ice-sheet thinning from around 270 m at 9.6 ka ([Bentley et al., 2011](#)). Similarly the onset of marine sedimentation in a nearby inundated lake basin at 19.41 m asl close to Parvenu Point at or before 8.8 cal ka BP provides a lower ice thickness constraint for the rapid deglaciation of Pourquois-Pas Island ([Hodgson et al., 2013](#)). Both age constraints support the interpretation of rapid thinning of the Marguerite Trough palaeo-ice stream at this time. This interpretation is also consistent with evidence from Alexander Island for the early Holocene loss of at least the northern part of the George VI Ice Shelf between ~9.6 cal ka and ~7.7 cal ka BP ([Bentley et al., 2005](#); [Hodgson et al., 2006](#); [Smith et al., 2007](#); [Roberts et al., 2009](#)). The break-up of the George VI Ice Shelf followed 500 m of thinning recorded at Ablation Point Massif and exposure of the Citadel Bastion summit (465.4 m altitude) at ~10.6 ka (Map ID 216; [Hodgson et al., 2009](#)). Within Calmette Bay, a small fjord along the eastern inland shores of Marguerite Bay, [Simkins et al. \(2013\)](#) identified two sets of raised beaches. The lower set are unequivocally Holocene in age and suggest minimum ages of open water within the small fjord at around 6.2 cal ka BP (Map ID 254; [Simkins et al., 2013](#)).

At 10 cal ka BP the grounding line in Biscoe Trough and Anvers-Hugo Trough must have been located somewhere inland of all dated cores (i.e. all the ages are >10 cal ka BP). On north-western Alexander Island, the ice was ~140 m thicker than at present ([Fig. 8](#)) ([Johnson et al., 2011](#)). In Adelaide Trough the grounding-line was located seaward of core GC01 in Lallemand Fjord, and ice-free conditions were established there by 9.2 ± 0.6 cal ka BP ([Shevenell et al., 1996](#); Map ID 56). Thus, the ice-front in this region is thought to have been in close-proximity to the present-day margin for the last 10 ka BP. An age of 8.4 ± 1.2 cal ka BP obtained from the AIO of transitional glaciomarine deposits in Gerlache-Boyd Strait may limit ice to the north of core site PC83 (Map ID 10), but its reliability is questionable, not only because of the problems associated with dating AIO, but also because the core sampled a lag deposit ([Harden et al., 1992](#)). Nevertheless, a large sill at the mouth of Gerlache Strait which is carpeted by morainic deposits on its southern flank, likely marks a significant pinning point during grounding-line retreat ([Heroy and Anderson, 2005](#)). An AIO age of 9.0 cal ka BP on the outer shelf of Orleans Trough (Map ID 30) also hints at a relatively seaward ice-margin position at the 10 ka BP time-slice ([Heroy and Anderson, 2007](#)), but as mentioned above, this age may be much younger than the actual timing of grounding-line retreat. Although the chronology of Orleans Trough is poorly resolved, the identification of a pebbly, stratified sandy mud overlying the subglacial till does imply deposition beneath an ice-shelf once the grounding-line had lifted off ([Heroy et al., 2008](#)).

Cosmogenic nuclide dating of glacial erratics indicate that Seymour Island and northern James Ross Island (Cape Lachman) were free of grounded ice by ~8 ka, and Terrapin Hill was ice-free by 6.8 ka ([Johnson et al., 2011](#); [Fig. 9](#); Map ID 158). Radiocarbon dates from glaciomarine sediments at The Naze (northern James Ross Island, [Fig. 9D](#)) indicate that Herbert Sound became free of grounded

ice between 6.3 and 7.8 ka BP (Hjort et al., 1997; Davies et al., 2012a). Cosmogenic ^3He dating of unmodified bedrock plateaux on western James Ross Island (i.e., Patalamon Mesa and Crisscross Crags; Fig. 7), suggests they were ice-free for a maximum of 15 ka during the past 4.69 million years, which probably included the past ~6.7 ka (Johnson et al., 2009). The ice cover was relatively thin (probably ≤ 200 m). Some ice probably also remained on flat-topped mesas for several hundred years after widespread deglaciation had occurred (Johnson et al., 2011). Cosmogenic nuclide dates on erratic boulders on Ulu Peninsula indicate that the ice configuration was similar to present by ~6 ka (Glasser et al., 2014).

In the South Shetland Islands, variations in sedimentation rates, carbon, silica and diatom contents in marine cores suggest ice retreated from Maxwell Bay in a stepwise manner from 14.1 to 8.2 cal ka BP, with particularly rapid retreat between 10.1 and 8.2 cal ka BP (Milliken et al., 2009). Inner Maxwell Bay was ice free by 9.1 cal ka BP and the entire bay was ice free by 5.9 cal ka BP, except for some smaller tributary fjords (Simms et al., 2011). On land there is evidence for progressive ice retreat, from cosmogenic exposure ages on glacially striated bedrock (Seong et al., 2009), the onset of lake sedimentation (Mäusbacher et al., 1989; Schmidt et al., 1990; Watcham et al., 2011) and formation of raised beaches (Barsch and Mäusbacher, 1986; Del Valle et al., 2002; Hall, 2010). Ice retreated from Fildes Peninsula, King George Island, between 11 and 9 cal ka BP, with glaciers being at or within their present limits by 6.1 cal ka BP (Mäusbacher, 1991; Watcham et al., 2011), and lake sedimentation commencing after this time (Tatur et al., 1999). At Potter Cove, ice recession was underway by c. 9.5 cal ka BP (Sugden and John, 1973). Lake sedimentation at Byers Peninsula, Livingston Island, seems to have started later, with a minimum age of c. 7.5 cal ka BP (Toro et al., 2013). However, further field studies of the transition between glacial and lacustrine sediments on Byers Peninsula are required.

4.5. 5 ka BP

Along the western AP there are, to date, no marine radiocarbon ages for the deglacial transition that are younger than 6.8 cal ka BP. This implies the ice sheet may have retreated almost to its present-day position by 5 cal ka BP, which is in agreement with the terrestrial data (Bentley et al., 2011) (Fig. 10). This includes the retreat of ice from the near-coastal part of Marguerite Bay (e.g. Allen et al., 2010; Kilfeather et al., 2011) and lift-off of grounded ice in George VI Sound and Eltanin Bay resulting in formation of the present ice-shelves (Sugden and Clapperton, 1981; Hjort et al., 2001; Smith et al., 2007; Hillenbrand et al., 2010a). On the north-western AP around Anvers Trough, the Bethelot islands were ice-free by 8.7 ka (160 m asl) and Primavera Station (40 m asl) became ice-free by 6.5 ka (Bentley et al., 2006). The ice-sheet margin was therefore located roughly in its present configuration along much of the western AP since the mid-Holocene, with the major phase of retreat having occurred between 15 and 10 ka BP as discussed above (Fig. 10).

Prince Gustav Channel is thought to have been free of grounded ice since the mid to late Holocene (Map IDs 44–45, Figs. 9 and 10); terrestrial cosmogenic nuclide ages on an ice-stream lateral moraine at Kaa Bluff on Ulu Peninsula, James Ross Island, indicate that this region of the channel was ice-free by 7.6 ka (Map ID 248; Fig. 9). Further south, the exact timing of ice sheet retreat in the trough remains a matter of debate due to the large uncertainty inherent in AIO ^{14}C dating in this area. Re-calibration of AIO ^{14}C ages from cores VC236, VC243 and VC244 suggest that the Prince Gustav Ice Shelf was absent between 6.8 and 1.8 cal ka BP, slightly earlier than previously reported (e.g., 5–2 ka BP in Pudsey and Evans, 2001). In the Larsen-A embayment, open-marine facies and clast

provenance in sediment cores suggest major retreat episodes of the Larsen-A Ice Shelf during the late Holocene (Domack et al., 2001; Brachfeld et al., 2003; Pudsey et al., 2006), probably between 3.8 and 1.4 cal ka BP (Brachfeld et al., 2003). In contrast, marine sedimentary sequences recovered further south do not indicate significant post-LGM reductions of the Larsen-B and Larsen-C ice shelves before 2002 (Domack et al., 2005; Curry and Pudsey, 2007).

The onshore record from the north-eastern AP has relatively little direct glacial geological data relating to ice sheet thickness and extent around ~5 ka. We know, however, that most of Ulu Peninsula on northern James Ross Island was free of grounded ice by ~6 ka (Glasser et al., 2014; Fig. 9B). Lake sedimentation began at Keyhole Lake 2 km inland of Brandy Bay before 4.6 ± 0.2 cal ka BP (Fig. 5B; Supplementary Data Table 4; Map IDs 90–91; Björck et al., 1996a), although there is low confidence in these ages, as the lake may have been contaminated with ancient carbon as it is fed by glacial meltwater (Hjort et al., 1997). To the north, at Hope Bay, lake sedimentation began from a minimum extrapolated age of ~7.1 cal ka BP (Zale, 1994; Sterken et al., 2012). Slightly farther south at Sjögren-Boydell and Drygalski Glaciers, the ice surface had lowered to near present sea level by 4 ka (Balco et al., 2013).

On the South Shetland Islands, tidewater glaciers retreated from the tributary fjords in Maxwell Bay from ca 4.5 to at least 2.8 cal ka BP (Map ID 74; Yoon et al., 2000), although ice may have persisted in small coves until 1.7 cal ka BP (Simms et al., 2011). Terrestrial evidence from lake sediments and moss banks suggests that during the latter part of the Holocene the climate ameliorated, with mild and humid conditions peaking between 3.0 and 2.8 cal ka BP (Björck et al., 1991a, 1991b, 1993, 1996b). Deglaciation of the shallow marine platform along the Admiralty Bay margin occurred ca 1.9–1.2 cal ka BP (Yoon et al., 2000).

Late Holocene glacial readvances are also recorded in several places around the AP and South Shetland Islands, and are probably a feature of most areas. For example, a large readvance of glacier IJR45 as recorded by moraines on James Ross Island occurred after 6.1 cal ka BP (terrestrial radiocarbon age; Map ID 80), and the glacier remained at this extended position until after ~4 ka (Rabassa, 1987; Björck et al., 1996a; Hjort et al., 1997; Davies et al., 2013). In addition, a readvance tentatively assigned to the Neoglaciation resulted in the presence of small, sharp crested moraines on James Ross Island, inferred to have ages of less than 1000 years (Carrivick et al., 2012; Davies et al., 2013), when a period of cooler climate was recorded in the James Ross Island Ice Core (Fig. 7B; Mulvaney et al., 2012). On Anvers Island, mosses overlain by a moraine suggest the presence of an ice advance after 700–970 cal yr BP (Hall et al., 2010b). In the South Shetlands Islands, readvance of glaciers occurred on King George Island during Neoglaciation cold events (Yoon et al., 2004; Yoo et al., 2009), for example between 0.45 and 0.25 cal ka BP (Simms et al., 2012).

Some late Holocene marine and terrestrial records from the South Shetland Islands indicate warmer temperatures between 1.4 and 0.55 cal ka BP and a cooler period at 0.55–0.05 cal ka BP, which have been tentatively linked to the northern hemisphere Medieval Warm Period and Little Ice Age (Fabrès et al., 2000; Khim et al., 2002; Liu et al., 2005; Hall, 2007; Hass et al., 2010; Monien et al., 2011; Majewski et al., 2012). Rapid regional warming and glacier retreat have occurred in the last 80 years (Vaughan et al., 2003; Yoo et al., 2009; Monien et al., 2011; Rückamp et al., 2011), at the same time as that observed along the western AP (Cook et al., 2005).

4.6. Twentieth Century

During the Twentieth Century, significant tidewater glacier recession has occurred on both sides of the AP in response to rapid atmospheric warming (Cook et al., 2005). The most recent estimate

of present day ice loss for the AP is -20 ± 16 Gt/yr, corresponding to a sea-level contribution of $+0.056 \pm 0.045$ mm/yr (Shepherd et al., 2012). The small AP peripheral island glaciers alone are losing around 7 ± 4 Gt yr⁻¹ of mass (Gardner et al., 2013). Around the northern tip of the AP, tidewater glaciers on the east side of the peninsula are shrinking faster than those on the west side, and small land-terminating glaciers on the northeast AP are also shrinking rapidly (Engel et al., 2012; Davies et al., 2012b).

AP tidewater glaciers are currently undergoing enhanced thinning and melting in their downstream sections (Kunz et al., 2012). The highest rates of surface lowering are found in the northwest AP and annual rates of thinning have accelerated to 0.6 m yr⁻¹ since the 1990s. This increase in frontal surface lowering corresponds well to observed increases in positive degree day sums (e.g., Barrand et al., 2013a). Thinning is not observed in the higher accumulation zones of these glaciers, where it may be offset by the high snow accumulation rates. The widespread glacier recession and thinning has been accompanied by flow acceleration, with the largest accelerations occurring on the glaciers receding most (Pritchard and Vaughan, 2007; Pritchard et al., 2009).

Ice shelves along the western and eastern AP are also shrinking and disintegrating in response to basal thinning and surface melt, with increased meltwater ponding on the surface during warm austral summers (Scambos et al., 2009; Pritchard et al., 2012; Rignot et al., 2013). Exceptionally high rates of basal melting are occurring beneath George VI Ice Shelf and the nearby Stange and Wilkins ice shelves, which lose nearly all their mass by basal melting. These small ice shelves along the coasts of the Bellingshausen and Amundsen seas (westwards to Getz Ice Shelf) account for nearly 48% of total meltwater production from Antarctic ice shelves, despite covering only 8% of the total Antarctic ice-shelf area (Rignot et al., 2013). Around 28,000 km² has been lost from AP ice shelves since 1960 (Cook and Vaughan, 2010), and the loss is occurring synchronously across the AP for the first time in the Holocene (Hodgson, 2011). The collapses of the Prince Gustav Channel ice shelf in 1995 and Larsen-B Ice Shelf in 2002 resulted in a number of immediate changes, including tributary glacier acceleration (Rignot et al., 2004; Scambos et al., 2004; Glasser et al., 2011), thinning (Scambos et al., 2004), and recession (Davies et al., 2012b).

So far, the largest southerly ice shelves on the western AP have not undergone disintegration on a scale similar to that observed on the north-eastern AP, and the George VI Ice Shelf in the early Holocene. However, the warming waters of the Bellingshausen Sea are contributing to the basal melting of George VI Ice Shelf (Holland et al., 2010), which is also speeding up concurrently with an increase in fracture extent and distribution (Holt et al., 2013). Wilkins Ice Shelf, west of Alexander Island, underwent large calving events in 2008 and 2009 following a period of thinning driven by high basal melt rates (Padman et al., 2012). Müller Ice Shelf, the most northerly ice shelf on the western AP, underwent substantial recession from 1986 to 1996, and has since remained relatively stable, at approximately 50% of the size it was in 1956 (Cook and Vaughan, 2010).

5. Numerical modelling of the Antarctic Peninsula Ice Sheet

Geological data, such as that summarised in this paper, can be used to drive numerical ice sheet models, thus deriving important information regarding ice volume, ice thickness, velocities, glacier dynamics and thermal regime. Numerous attempts, of varying degrees of complexity, have recently been made at modelling the Antarctic Ice Sheet through the LGM (Denton and Hughes, 2002; Huybrechts, 2002; Ivins and James, 2005; Bentley et al., 2010; Le Brocq et al., 2011; Pollard and DeConto, 2012; Golledge et al.,

2012a,b, 2013; Whitehouse et al., 2012a). Numerical models are constantly improved by the increasingly high-resolution BEDMAP 2 dataset (Fretwell et al., 2013), better constraints on present conditions, surface mass balance (Shepherd et al., 2012) and ice flow velocities (Rignot et al., 2011), as well as improved geological reconstructions of past ice-sheet extent and thickness (e.g., this special issue). These data, combined with high-resolution swath bathymetry, can be used to provide insights into specific ice-stream recession. For example, Jamieson et al. (2012, 2014) use the geomorphological record to explore marine ice stream instability for the Marguerite Bay Ice Stream using a high resolution flowline model.

Three dimensional thermomechanical ice sheet models such as Glimmer (Rutt et al., 2009) or PISM (Golledge et al., 2012a,b) can be used to investigate palaeo ice-sheet dynamics across the entire ice sheet during the LGM. The narrow mountain chain of the Antarctic Peninsula has proven difficult to model, as coarser models are unable to resolve the underlying bedrock topography (Whitehouse et al., 2012a). However, the GLIMMER model (Whitehouse et al., 2012a) reproduces a thick ice sheet along the Antarctic Peninsula at 20 ka, with nunataks being covered by ice.

A recent attempt using a high-resolution (5 km) ice sheet model (PISM) (Golledge et al., 2012a,b, 2013) was able to evolve more complex flow pathways. The 5 km resolution PISM reconstruction suggests that during the LGM, the thin ice along the spine of mountains along the Antarctic Peninsula was cold-based and below pressure melting point, which agrees with observations from ice-rafted debris (Reinardy et al., 2009), whereas ice on the continental shelf was at the pressure melting point. It matches geological data in many ways; for example, the model shows a dome forming over James Ross Island during the LGM, suggesting that the Mount Haddington Ice Cap was not overridden, which agrees with observations (Davies et al., 2012a). This model also generates nunataks on the higher summits of Alexander Island, constraining ice-sheet thickness. Ice stream velocities reach 200 m a⁻¹ for the eastern outlets. Mismatches occur in several areas of the continental shelf, but modelled flow-lines broadly agree with reconstructed ice-flow directions (Golledge et al., 2013).

Numerical modelling crucially allows predictions to be made about the future of the APIS. Improved observations of ice velocities, bedrock topography and bathymetry and surface mass balance have allowed the development of a new generation of ice sheet models, which compute ice fluxes from these observational data. These models anticipate grounding-line migration as a result of future ice-shelf collapse, which reduces buttressing forces and leads to recession (Barrand et al., 2013b). These models allow the volume response of a 10 and 20 km grounding line retreat or surface mass balance anomalies to be analysed.

Over the next 200 years, the sea level contribution from the APIS is expected to be negative, as increased accumulation offsets higher temperatures and increased melting (Barrand et al., 2013b). However, increased accumulation also results in increased ice discharge, which returns ~30% of the mass gained to the ocean by 2200 AD. Grounding line retreats of 10 km imposed on each of the 20 largest drainage basins resulted in a variable volume response, with some basins contributing up to 1.5 mm of sea level rise. However, several basins showed little or no change after 200 years. A grounding line retreat of 20 km resulted in a volume response of up to 0.5–3 mm of sea level equivalent (SLE) per basin (Barrand et al., 2013b).

As 19 of the largest drainage basins terminate in ice shelves, the cumulative effect of ice-shelf collapse across the APIS was calculated. If all ice shelves are removed by the year 2020 AD, the dynamic response of the entire APIS was 7–25 mm SLE by 2100 AD and 8–32 mm by 2200 AD, depending on whether a 10 or 20 km grounding line recession is imposed (Barrand et al., 2013b). The

maximum possible volume response is unlikely to exceed 50 mm SLE by 2200 AD, even with a 20 km grounding-line retreat scenario. Ultimately, [Barrand et al., 2013b](#) conclude that values of 10–20 mm SLE from grounding line retreat alone seem plausible.

6. Discussion

Marine geological and geophysical datasets from the AP continental margin provide strong evidence that the APIS was grounded at, or close to, the shelf edge at the LGM (25–20 ka BP). This evidence comprises subglacial tills in sediment cores and a range of subglacial landforms, including MSGs, drumlins and grooved bedrock, as well as GZWs. Typically, the outer shelf is floored by a soft unconsolidated substrate in which MSGs are well developed, while the inner shelf comprises a generally rougher terrain of locally ice-moulded crystalline bedrock dissected in places by subglacial meltwater channels, with localised till patches. Based on the distribution of glacial landforms, particularly MSGs, the APIS is known to have been drained by a series of palaeo-ice streams flowing through cross-shelf bathymetric troughs around the Peninsula. On the western Peninsula in particular, numerous offshore islands acted as topographic barriers to flow, guiding ice streams into ever deeper pre-existing bathymetric troughs ([Golledge et al., 2013](#)). These palaeo-ice streams were probably surrounded by slower moving ice on the intervening shallower, and commonly iceberg scoured, banks ([Fig. 11](#)) (cf. [Dowdeswell et al., 2004a](#); [Evans et al., 2005](#); [Heroy and Anderson, 2005](#); [Ó Cofaigh et al., 2008](#); [Livingstone et al., 2012](#); [Davies et al., 2012a](#)). Subglacial tills range from stiff over-consolidated diamictos which have been recovered in cores from both inside and outside of bathymetric troughs, to soft porous diamictos that are found in cores from within troughs; MSGs are typically constructed from this soft till ([Evans et al., 2005](#); [Ó Cofaigh et al., 2005, 2007](#); [Reinardy et al., 2011a,b](#); [Livingstone et al., 2012](#)). The soft tills and associated MSGs record streaming flow along the troughs at the LGM, and likely immediately after. Although GZWs have been recorded at the shelf edge/outer shelf in some locations, their absence in other areas implies that subglacial sediment advected to the grounding line was delivered directly onto the slope and remobilised as mass flows (e.g., [Vanneste and Larter, 1995](#); [Dowdeswell et al., 2004b](#); [Evans et al., 2005](#); [Amblas et al., 2006](#)).

Although the existing data indicate that a grounded APIS extended to the shelf edge or outer shelf around much of the peninsula at the LGM, significant data gaps remain, most notably on the Weddell Sea margin of the eastern AP (see also [Hillenbrand et al.](#) this volume), and also at the northern tip of the AP. Based on the terrestrial and marine data, we are currently unable to distinguish any change in ice sheet extent between 25 and 20 cal ka BP and so we infer that the ice sheet was still at its maximum extent at 20 cal ka BP. This suggests that the ice sheet was grounded at the shelf edge for several thousand years at least in some areas, although some ice streams, such as the one in Marguerite Trough ([Ó Cofaigh et al., 2005](#)) may have been short-lived, non-steady state features. Given the paucity of dates constraining the advance of grounded ice across the shelf, the timing and duration during which the APIS reached its maximum extent remains unresolved. However, records from Horseshoe Island in inner Marguerite Bay suggest that mosses were present on land at 28.8 ± 0.28 cal ka BP, limiting ice thickness there to 80–140 m above present sea level ([Hodgson et al., 2013](#)).

Dates from Vega Trough indicate that the ice sheet had retreated from the shelf edge by 18.3 cal ka BP ([Heroy and Anderson, 2007](#)). The transition from grounded to floating ice in the former Larsen-A region occurred at 10.6–10.7 cal ka BP based on RPI and AMS radiocarbon dating ([Brachfeld et al., 2003](#); [Domack et al., 2005](#)), but

it appears to have been earlier (13.6 cal ka BP) in Prince Gustav Channel ([Pudsey and Evans et al., 2005](#); [Pudsey et al., 2006](#)). In the northeast AP, the Firth of Tay deglaciated around ~9.4 cal ka BP ([Michalchuk et al., 2009](#)). In the west, ages for initial retreat from the outer shelf decrease both from the outer to inner shelf, and also from north to south along the peninsula. Retreat from the outer shelf was underway by 17.5 cal ka BP in Bransfield Basin, while further south in Anvers Trough and Marguerite Trough, initial ice retreat may not have occurred until 15–16 cal ka BP and 14 cal ka BP, respectively ([Heroy and Anderson, 2007](#); [Kilfeather et al., 2011](#)). Terrestrial evidence from Marguerite Bay indicates that ice sheet thinning was already underway by 18 ka ([Bentley et al., 2011](#)).

Recession of individual ice streams across the western AP shelf was therefore asynchronous between troughs in terms of the timing of initial grounding line recession. However, subsequent retreat rates also seem to exhibit marked spatial variations, if we assume that the deglaciation ages are close to the true time of grounding-line retreat, i.e. that the fact that the dates are minimum ages has not significantly altered the timing of palaeo-ice stream retreat. For example, according to the core chronologies from Anvers Trough grounding-line retreat was initially slow across the outer-mid shelf (mean retreat rates of 2–15 m yr⁻¹) but then accelerated (47 m yr⁻¹) ([Heroy and Anderson, 2007](#); [Livingstone et al., 2012](#)). By contrast, in Marguerite Trough, retreat across the outer shelf was rapid with mean retreat rates of ~80 m yr⁻¹, although these rates could have been considerably greater given the overlap in the error of dates constraining retreat along a 140 km long stretch of the outer to mid-shelf part of the trough ([Kilfeather et al., 2011](#)). Variations in retreat style and rate between individual troughs are also implied from the mapped glacial geomorphology. The distribution of GZWs, which often overprint or disrupt MSGs on the shelf, indicates the occurrence of temporary stillstands or slow-downs in the rate of grounding line retreat in the bathymetric troughs, and show that post-LGM grounding-line retreat ranged from continuous to episodic ([Larter and Vanneste, 1995](#); [Heroy and Anderson, 2007](#); [Ó Cofaigh et al., 2008](#); [Livingstone et al., 2012, 2013](#)). Retreat in some troughs was interrupted by a series of re-advances and ice-shelf breakup and reformation episodes (e.g., Prince Gustav Channel; [Pudsey and Evans, 2001](#)). The presence of GZWs indicating episodic retreat contrasts with areas characterised by uninterrupted MSGs and where GZWs are absent, implying continuous, possibly rapid retreat ([Ó Cofaigh et al., 2008](#); [Dowdeswell et al., 2008](#)). Although GZWs can also form as the grounding line advances across the shelf, such GZWs are likely to be successively eroded or substantially modified when they are overridden by the advancing ice. Retreat from the inner shelf was strongly diachronous, with dates ranging from 13 to 7 cal ka BP ([Heroy and Anderson, 2007](#)). As suggested by [Heroy and Anderson \(2007\)](#), this variability may reflect the influence of local controls on retreat rate; notably the rugged, bedrock dominated, inner shelf which would have facilitated pinning on bedrock highs and topographic constrictions.

This influence of seafloor (subglacial) topography on retreat rates is exemplified by the case of Marguerite Trough. There, radiocarbon dates from a 140 km long section of the outer shelf document a period of rapid palaeo-ice stream retreat ([Pope and Anderson, 1992](#); [Kilfeather et al., 2011](#)) in an area where a series of GZWs have been mapped on a reverse bed slope ([Jamieson et al., 2012, 2014](#); [Livingstone et al., 2013](#)). This is interesting because it demonstrates that GZWs, typically regarded as being indicators of grounding-line stabilisation or slow down ([Dowdeswell and Fugelli, 2012](#)), can develop on a reverse bed slope. [Jamieson et al.](#)

(2012) have shown how retreat rates and transient pauses in grounding line recession on the reverse bed slope of Marguerite Trough are associated with constrictions in trough width along the ice-stream flow path, which caused enhanced lateral drag as the ice stream narrowed. In conjunction with shallower areas in the trough, such pinning points emphasise the importance of along-flow variations in subglacial topography as a mechanism for modulating the discharge of individual APIS outlets.

7. Conclusions

- This paper is a reconstruction of the changing extent and configuration of the APIS from LGM to present. The reconstruction is underpinned chronologically by a database of radiocarbon ages on glaciomarine sediments, lake and terrestrial organic remains, and cosmogenic nuclide surface exposure ages on erratics and bedrock. The resulting ice sheet retreat history, particularly along the western AP continental shelf, is one of the best constrained in Antarctica.
- The APIS was grounded on the outer shelf/at the shelf edge of the peninsula at the LGM and remained there until ~20 ka BP. The ice sheet was drained by a series of palaeo-ice streams that extended across the continental shelf via bathymetric troughs.
- Initial ice sheet retreat in the east was underway by about 18 cal ka BP. The earliest dates on retreat in the west are from Bransfield Basin and show that retreat there was underway by 17.5 cal ka BP. The timing of the onset of initial retreat decreased southwards along the western AP shelf with the large ice stream in Marguerite Trough remaining grounded at the shelf edge until about 14 cal ka BP, although thinning was underway by 18 ka BP.
- Ice streams remained active during deglaciation at least until the ice sheet had pulled back to the mid-shelf. They left a strong geomorphological and sedimentary imprint within the cross-shelf bathymetric troughs in the form of flow-parallel, stream-lined subglacial landforms, GZWs and subglacial tills.
- Retreat was asynchronous between individual troughs and subglacial topography exerted a major control on retreat. In some troughs the grounding-line retreat slowed or paused on reverse bed slopes during deglaciation.
- Between 15 and 10 cal ka BP the APIS underwent significant recession along the western AP margin. In Marguerite Trough the ice sheet may have still been grounded on the mid-shelf at 10 cal ka BP. In the Larsen-A region the transition from grounded to floating ice was established by 10.7–10.6 cal ka BP.
- The APIS had retreated towards its present configuration in the western AP by the mid-Holocene and may have approached its present configuration on the eastern AP margin several thousand years earlier at the start of the Holocene. Subsequent mid to late-Holocene retreat was diachronous.
- Although the LGM configuration and subsequent retreat history of the APIS is relatively well known compared to other regions of Antarctica, there remain significant gaps in terms of data coverage (e.g., the Weddell Sea margin of the AP) and understanding (e.g., whether there were significant mid-Holocene readvances). Even in comparatively well studied areas, such as the Larsen-A region and troughs on the western AP shelf, existing ages on ice sheet retreat are often sparse or not fully reliable reflecting, for example, contamination by fossil carbon or a scarcity of calcareous (micro-) fossils. An improved chronology of both grounding line retreat in individual troughs and outlet glacier thinning histories from cosmogenic nuclide dating is essential to determine retreat rates and assess variability between different glacial catchments. Such data are also critical constraints on numerical ice-sheet models which seek to

determine the controls on ice stream retreat, particularly in areas of reverse bed slope.

Acknowledgements

This review is a contribution to the 'Reconstruction of Antarctic Ice Sheet Deglaciation' project which is supported by the Scientific Committee for Antarctic Research Antarctic Climate Evolution Programme (SCAR-ACE). The research that underpins this review was supported in numerous grants over many years awarded through various funding agencies but notably the UK Natural Environment Research Council (NERC), the USA National Science Foundation (Office of Polar Programs), the Spanish National Antarctic Program and MINECO Polar Research Area, and the Catalan government.

Appendix A. Supplementary data

Supplementary data related to this article can be found at <http://dx.doi.org/10.1016/j.quascirev.2014.06.023>.

References

- Allen, C.S., Oakes-Fretwell, L., Anderson, J.B., Hodgson, D.A., 2010. A record of Holocene glacial and oceanographic variability in Neny Fjord, Antarctic Peninsula. *Holocene* 20, 551–564.
- Amblas, D., Urgeles, R., Canals, M., Calafat, A.M., Rebesco, M., Camerlenghi, A., Estrada, F., De Batist, M., Hughes-Clarke, J.E., 2006. Relationship between continental rise development and palaeo-ice sheet dynamics, Northern Antarctic Peninsula Pacific margin. *Quat. Sci. Rev.* 25, 933–944.
- Anderson, J.B., Shipp, S.S., Lowe, A.L., Wellner, J.S., Mosola, A.B., 2002. The Antarctic Ice Sheet during the Last Glacial Maximum and its subsequent retreat history: a review. *Quat. Sci. Rev.* 21, 49–70.
- Anderson, J.B., Oakes-Fretwell, L., 2008. Geomorphology of the onset area of a palaeo-ice stream, Marguerite Bay, Antarctica Peninsula. *Earth Surf. Process. Landf.* 33, 503–512.
- Andrews, J.T., Domack, E.W., Cunningham, W.L., Leventer, A., Licht, K.J., Jull, A.J.T., DeMaster, D.J., Jennings, A.E., 1999. Problems and possible solutions concerning radiocarbon dating of surface marine sediments, Ross Sea, Antarctica. *Quat. Res.* 52, 206–216.
- Applegate, P.J., Urban, N.M., Keller, K., Lowell, T.V., Laabs, B.J.C., Kelly, M.A., Alley, R.B., 2012. Improved moraine age interpretations through explicit matching of geomorphic process models to cosmogenic nuclide measurements from single landforms. *Quat. Res.* 77, 293–304.
- Balco, G., Stone, J.O., Lifton, N.A., Dunai, T.J., 2008. A complete and easily accessible means of calculating surface exposure ages or erosion rates from ¹⁰Be and ²⁶Al measurements. *Quat. Geochronol.* 3, 174–195.
- Balco, G.A., 2011. Contributions and unrealized potential contributions of cosmogenic-nuclide exposure dating to glacier chronology, 1990–2010. *Quat. Sci. Rev.* 30, 3–27.
- Balco, G.A., Schaefer, J.M., LARISSA Group, 2013. Terrestrial exposure-age record of Holocene ice sheet and ice-shelf change in the northeast Antarctic Peninsula. *Quat. Sci. Rev.* 59, 101–111.
- Banfield, L.A., Anderson, J.B., 1995. Seismic facies investigation of the Late Quaternary glacial history of Bransfield Basin, Antarctica. In: Cooper, A.K., et al. (Eds.), *Geology and Seismic Stratigraphy of the Antarctic Margin*, Antarctic Research Series, vol. 68. AGU, Washington, pp. 123–140.
- Barrand, N.E., Hindmarsh, R.C.A., Arthern, R., Williams, C.R., Mougnot, J., Scheuchl, B., Rignot, E., Ligtenberg, S.R.M., van den Broeke, M.R., Edwards, T.L., Cook, A.J., Simonsen, S.B., 2013b. Computing the volume response of the Antarctic Peninsula Ice Sheet to warming scenarios to 2200. *J. Glaciol.* 59 (215), 397–409.
- Barrand, N.E., Vaughan, D.G., Steiner, N., Tedesco, M., Kuipers Munneke, P., van den Broeke, M.R., Hosking, J.S., 2013a. Trends in Antarctic Peninsula surface melting conditions from observations and regional climate modelling. *J. Geophys. Res.* 118, 1–16.
- Barsch, D., Mäusbacher, R., 1986. New data on the relief development of the South Shetland Islands, Antarctica. *Interdiscip. Sci. Rev.* 11, 211–218.
- Bart, P.J., Anderson, J.B., 1995. Seismic record of glacial events affecting the Pacific margin of the northwestern Antarctic Peninsula. In: Cooper, A.K., et al. (Eds.), *Geology and Seismic Stratigraphy of the Antarctic Margin*, Antarctic Research Series, vol. 68. AGU, Washington, pp. 75–95.
- Bentley, M.J., Anderson, J.B., 1998. Glacial and marine geological evidence for the extent of grounded ice in the Weddell Sea-Antarctic Peninsula region during the Last Glacial Maximum. *Antarct. Sci.* 10, 307–323.
- Bentley, M.J., Hodgson, D.A., Smith, J.A., Cox, N.J., 2005. Relative sea level curves for the South Shetland Islands and Marguerite Bay, Antarctic Peninsula. *Quat. Sci. Rev.* 24, 1203–1216.

- Bentley, M.J., Fogwill, C.J., Kubnik, P.W., Sugden, D.E., 2006. Geomorphological evidence and cosmogenic $^{10}\text{Be}/^{26}\text{Al}$ exposure ages for the Last Glacial Maximum and deglaciation of the Antarctic Peninsula Ice Sheet. *Geol. Soc. Am. Bull.* 118, 1149–1159.
- Bentley, M.J., Hodgson, D.A., Smith, J.A., Ó Cofaigh, C., Domack, E.W., Larter, R.D., Roberts, S.J., Brachfeld, S., Leventer, A., Hjort, C., Hillenbrand, C.-D., Evans, J., 2009. Mechanisms of Holocene palaeoenvironmental change in the Antarctic Peninsula region. *Holocene* 19, 51–69.
- Bentley, M.J., Fogwill, C.J., Le Brocq, A.M., Hubbard, A.L., Sugden, D.E., Dunai, T.J., Freeman, S.P.H.T., 2010. Deglacial history of the West Antarctic Ice Sheet in the Weddell Sea Embayment: constraints on past ice volume change. *Geology* 38, 411–414.
- Bentley, M.J., Johnson, J.S., Hodgson, D.A., Dunai, T., Freeman, S.P.H.T., Ó Cofaigh, C., 2011. Rapid deglaciation of Marguerite Bay, western Antarctic Peninsula in the Early Holocene. *Quat. Sci. Rev.* 30, 3338–3349.
- Berkman, P.A., Andrews, J.T., Björck, S., Colhoun, E.A., Emslie, S.D., Goodwin, I.D., Hall, B.L., Hart, C.P., Hirakawa, K., Igarashi, A., Ingólfsson, O., López-Martínez, J., Lyons, W.B., Mabin, M.C.G., Quilty, P.G., Taviani, M., Yoshida, Y., 1998. Circum-Antarctic coastal environmental shifts during the Late Quaternary reflected by emerged marine deposits. *Antarct. Sci.* 10 (03), 345–362.
- Björck, S., Håkansson, H., Zale, R., Karlén, W., Jönsson, B.L., 1991a. A late Holocene lake sediment sequence from Livingston Island, South Shetland Islands, with palaeoclimatic implications. *Antarct. Sci.* 3, 61–72.
- Björck, S., Malmer, N., Hjort, C., Sandgren, P., Ingólfsson, Ó., Wallen, B., Smith, R.I.L., Jönsson, B.L., 1991b. Stratigraphic and paleoclimatic studies of a 5500-year-old moss bank on Elephant Island, Antarctica. *Arct. Alp. Res.* 23, 361–374.
- Björck, S., Håkansson, H., Olsson, S., Barnekow, L., Janssens, J., 1993. Palaeoclimatic studies in South Shetland Islands, Antarctica, based on numerous stratigraphic variables in lake sediments. *J. Paleolimnol.* 8, 233–272.
- Björck, S., Olsson, S., Ellis-Evans, C., Håkansson, H., Humlum, O., de Lirio, J.M., 1996a. Late Holocene palaeoclimatic records from lake sediments on James Ross Island, Antarctica. *Palaeogeogr. Palaeoclimatol. Palaeoecol.* 121, 195–220.
- Björck, S., Hjort, C., Ingólfsson, Ó., Zale, R., Ising, J., 1996b. Holocene deglaciation chronology from lake sediments. In: López-Martínez, J., Thomson, M.R.A., Arche, A., Björck, S., Ellis-Evans, J.C., Hathway, B., Hernández-Cifuentes, F., Hjort, C., Ingólfsson, Ó., Ising, J., Lomas, S., Martínez de Pison, E., Serrano, E., Zale, R., King, S. (Eds.), *Geomorphological Map of Byers Peninsula, Livingston Island*. British Antarctic Survey, Cambridge, pp. 49–51. Sheet 45-A, 41:25 000 with supplementary text.
- Brachfeld, S.A., Banerjee, S.K., Guyodo, Y., Acton, G.D., 2002. A 13,200 year history of century to millennial-scale paleoenvironmental change magnetically recorded in the Palmer Deep, western Antarctic Peninsula. *Earth Planet. Sci. Lett.* 194, 311–326.
- Brachfeld, S., Domack, E.W., Kissel, C., Laj, C., Leventer, A., Ishman, S., Gilbert, R., Camerlenghi, A., Eglinton, L.B., 2003. Holocene history of the Larsen-A Ice Shelf constrained by geomagnetic paleointensity dating. *Geology* 31, 749–752.
- Briggs, R.D., Tarasov, L., 2013. How to evaluate model-derived deglaciation chronologies: a case study using Antarctica. *Quat. Sci. Rev.* 63, 109–127.
- Camerlenghi, A., Domack, E., Rebesco, M., Gilbert, R., Ishman, S., Leventer, A., Brachfeld, S., Drake, A., 2001. Glacial morphology and post-glacial contourites in northern Prince Gustav Channel (NW Weddell Sea, Antarctica). *Mar. Geophys. Res.* 22, 417–443.
- Canals, M., Urgeles, R., Calafat, A.M., 2000. Deep sea-floor evidence of past ice streams off the Antarctic Peninsula. *Geology* 28, 31–34.
- Canals, M., Casamor, J.L., Urgeles, R., Calafat, A.M., Domack, E.W., Baraza, J., Farran, M., De Batist, M., 2002. Sea-floor evidence of a subglacial sedimentary system off the northern Antarctic Peninsula. *Geology* 30, 603–606.
- Canals, M., Calafat, A., Camerlenghi, A., De Batist, M., Urgeles, R., Farran, M., Gettler, R., Versteeg, W., Amblas, D., Rebesco, M., Casamor, J.L., Sanchez, A., Willmott, V., Lastras, G., Imbo, Y., 2003. Uncovering the footprint of former ice streams off Antarctica. *Eos* 84 (11), 97–103.
- Carrivick, J.L., Davies, B.J., Glasser, N.F., Nývlt, D., 2012. Late Holocene changes in character and behaviour of land-terminating glaciers on James Ross Island, Antarctica. *J. Glaciol.* 58, 1176–1190.
- Clapperton, C.M., Sugden, D.E., 1982. Late Quaternary glacial history of George VI Sound area, West Antarctica. *Quat. Res.* 18, 243–267.
- Collins, L.G., Pike, J., Allen, C.S., Hodgson, D.A., 2012. High resolution reconstruction of southwest Atlantic sea-ice and its role in the carbon cycle during marine isotope stages 3 and 2. *Palaeoceanography* 27, PA3217.
- Cook, A.J., Vaughan, D.G., 2010. Overview of areal changes of the ice shelves on the Antarctic Peninsula over the past 50 years. *Cryosphere* 4, 77–98.
- Cook, A.J., Fox, A.J., Vaughan, D.G., Ferrigno, J.G., 2005. Retreating glacier fronts on the Antarctic Peninsula over the past half-century. *Science* 308, 541–544.
- Curry, P., Pudsey, C.J., 2007. New Quaternary sedimentary records from near the Larsen C and former Larsen B ice shelves; evidence for Holocene stability. *Antarct. Sci.* 19, 355–364.
- Davies, B.J., Hambrey, M.J., Smellie, J.L., Carrivick, J.L., Glasser, N.F., 2012a. Antarctic Peninsula Ice Sheet evolution during the Cenozoic Era. *Quat. Sci. Rev.* 31, 30–66.
- Davies, B.J., Carrivick, J.L., Glasser, N.F., Hambrey, M.J., Smellie, J.L., 2012b. Variable glacier response to atmospheric warming, northern Antarctic Peninsula, 1888–2009. *Cryosphere* 6, 1031–1048.
- Davies, B.J., Glasser, N.F., Carrivick, J.L., Hambrey, M.J., Smellie, J.L., Nývlt, D., 2013. Landscape evolution and ice-sheet behaviour in a semi-arid polar environment: James Ross Island, NE Antarctic Peninsula. In: Hambrey, M.J., Barker, P.F., Barrett, P.J., Bowman, V.C., Davies, B.J., Smellie, J.L., Tranter, M. (Eds.), *Antarctic Palaeoenvironments and Earth Surface Processes*, Geological Society of London, Special Publications, vol. 381, pp. 1–43. London.
- De Angelis, H., Skvarca, P., 2003. Glacier surge after ice shelf collapse. *Science* 299, 1560–1562.
- Del Valle, R.A., Montalti, D., Inbar, M., 2002. Mid-Holocene macrofossil-bearing raised marine beaches at Potter Peninsula, King George Island, South Shetland Islands. *Antarct. Sci.* 14, 263–269.
- Denton, G.H., Hughes, T.J., 2002. Reconstructing the Antarctic Ice Sheet at the Last Glacial Maximum. *Quat. Sci. Rev.* 21, 193–202.
- Domack, E.W., 1992. Modern carbon-14 ages and reservoir corrections for the Antarctic Peninsula and Gerlache Strait area. *Antarct. J. U.S.* 27, 63–64.
- Domack, E.W., Jacobson, E.A., Shipp, S., Anderson, J.B., 1999. Late Pleistocene–Holocene retreat of the West Antarctic Ice-Sheet system in the Ross Sea: part 2—sedimentologic and stratigraphic signature. *Geol. Soc. Am. Bull.* 111 (10), 1517–1536.
- Domack, E.W., Leventer, A., Dunbar, G.B., Taylor, F., Brachfeld, S., Sjunneskog, C., Party, O.L.S., 2001. Chronology of the Palmer Deep site, Antarctic Peninsula: a Holocene palaeoenvironmental reference for the circum-Antarctic. *Holocene* 11, 1–9.
- Domack, E., Burnett, A., Leventer, A., 2003. Environmental setting of the Antarctic Peninsula. In: Domack, E., Leventer, A., Burnett, A., Bindshadler, R., Convey, P., Kirby, M. (Eds.), *Antarctic Peninsula Climate Variability: Historical and Paleoenvironmental Perspectives*, Antarctic Research Series, vol. 79. American Geophysical Union, Washington, pp. 1–13.
- Domack, E., Duran, D., Leventer, A., Ishman, S., Doane, S., McCallum, S., Amblas, D., Ring, J., Gilbert, R., Prentice, M., 2005. Stability of the Larsen B ice shelf on the Antarctic Peninsula during the Holocene epoch. *Nature* 436, 681–685.
- Domack, E.W., Amblas, D., Gilbert, R., Brachfeld, S., Camerlenghi, A., Rebesco, M., Canals, M., Urgeles, R., 2006. Subglacial morphology and glacial evolution of the Palmer deep outlet system, Antarctic Peninsula. *Geomorphology* 75, 125–142.
- Dowdeswell, J.A., Fugelli, E.M.G., 2012. The seismic architecture and geometry of grounding-zone wedges formed at the marine margins of past ice sheets. *Geol. Soc. Am. Bull.* 124, 1750–1761.
- Dowdeswell, J.A., Ó Cofaigh, C., Pudsey, C.J., 2004a. Thickness and extent of the subglacial till layer beneath an Antarctic palaeo-ice stream. *Geology* 32, 13–16.
- Dowdeswell, J.A., Ó Cofaigh, C., Evans, J., 2004b. Continental slope morphology and sedimentary processes at the mouth of an Antarctic palaeo-ice stream. *Mar. Geol.* 204, 203–214.
- Dowdeswell, J.A., Ottesen, D., Evans, J., Ó Cofaigh, C., Anderson, J.B., 2008. Submarine glacial landforms and rates of ice-stream collapse. *Geology* 36, 819–822.
- Engel, Z., Nývlt, D., Láska, K., 2012. Ice thickness, areal and volumetric changes of Davies Dome and Whisky Glacier in 1979–2006 (James Ross Island, Antarctic Peninsula). *J. Glaciol.* 58, 904–914.
- EPICA, 2006. One-to-one coupling of glacial climate variability in Greenland and Antarctica. *Nature* 444.
- Evans, J., Dowdeswell, J.A., Ó Cofaigh, C., 2004. Late Quaternary submarine bedforms and ice-sheet flow in Gerlache Strait and on the adjacent continental shelf, Antarctic Peninsula. *J. Quat. Sci.* 19, 397–407.
- Evans, J., Pudsey, C.J., Ó Cofaigh, C., Morris, P.W., Domack, E.W., 2005. Late Quaternary glacial history, dynamics and sedimentation of the eastern margin of the Antarctic Peninsula Ice Sheet. *Quat. Sci. Rev.* 24, 741–774.
- Fabrés, J., Calafat, A., Canals, M., Bárcena, M.A., Flores, J.A., 2000. Bransfield Basin fine-grained sediments: late-Holocene sedimentary processes and Antarctic oceanographic conditions. *Holocene* 10, 703–718.
- Fernandez-Carazo, R., Verleyen, E., Hodgson, D.A., Roberts, S.J., Waleron, K., Vyverman, W., Wilmotte, A., 2013. Late Holocene changes in cyanobacterial community structure in Maritime Antarctic lakes. *J. Paleolimnol.* <http://dx.doi.org/10.1007/s10933-013-9700-3>.
- Fink, D., McKelvey, B., Hambrey, M.J., Fabel, D., Brown, R., 2006. Pleistocene deglaciation chronology of the Amery Oasis and Radok Lake, northern Prince Charles Mountains, Antarctica. *Earth Planet. Sci. Lett.* 243, 229–243.
- Fretwell, P.T., Hodgson, D.A., Watcham, E., Bentley, M.J., Roberts, S.J., 2010. Holocene isostatic uplift of the South Shetland Islands, Antarctic Peninsula, modelled from raised beaches. *Quat. Sci. Rev.* 29, 1880–1893.
- Fretwell, P., plus 55 others, 2013. Bedmap2: improved ice bed, surface and thickness datasets for Antarctica. *Cryosphere* 7, 375–393.
- Gardner, A.S., plus 15 others, 2013. A reconciled estimate of glacier contributions to sea level rise: 2003 to 2009. *Science* 340, 852–857.
- Glasser, N.F., Scambos, T.A., Bohlander, J.A., Truffer, M., Pettit, E.C., Davies, B.J., 2011. From ice-shelf tributary to tidewater glacier: continued rapid glacier recession, acceleration and thinning of Röhss Glacier following the 1995 collapse of the Prince Gustav Ice Shelf on the Antarctic Peninsula. *J. Glaciol.* 57, 397–406.
- Glasser, N.F., Davies, B.J., Carrivick, J.L., Ródes, A., Hambrey, M.J., Smellie, J.L., Domack, E., 2014. Deglacial ice sheet thinning and ice-stream initiation on James Ross Island, northern Antarctic Peninsula. *Quat. Sci. Rev.* 86, 78–88.
- Golledge, N.R., Fogwill, C.J., Mackintosh, A.N., Buckley, K.M., 2012a. Dynamics of the last glacial maximum Antarctic ice-sheet and its response to ocean forcing. *Proc. Natl. Acad. Sci.* 109, 16052–16056.
- Golledge, N.R., Mackintosh, A.N., Anderson, B.M., Buckley, K.M., Doughty, A.M., Barrell, D.J.A., Denton, G.H., Vandergoes, M.J., Andersen, B.G., Schaefer, J.M., 2012b. Last Glacial Maximum climate in New Zealand inferred from a modelled Southern Alps icefield. *Quat. Sci. Rev.* 46, 30–45.
- Golledge, N.R., Levy, R.H., McKay, R.M., Fogwill, C.J., White, D.A., Graham, A.G.C., Smith, J.A., Hillenbrand, C.-D., Licht, K.J., Denton, G.H., Ackert Jr., R.P., Mass, S.M., Hall, B.L., 2013. Glaciology and geological signature of the Last Glacial Maximum Antarctic Ice Sheet. *Quat. Sci. Rev.* 78, 225–247.

- Graham, A.G.C., Smith, J.A., 2012. Palaeoglaciology of the Alexander Island ice cap, western Antarctic Peninsula, reconstructed from marine geophysical and core data. *Quat. Sci. Rev.* 35, 63–81.
- Hall, B.L., 2007. Late-Holocene advance of the Collins Ice Cap, King George Island, South Shetland Islands. *Holocene* 17, 1253–1258.
- Hall, B.L., 2010. Holocene relative sea-level changes and ice fluctuations in the South Shetland Islands. *Glob. Planet. Change* 74, 15–26.
- Hall, B.L., Henderson, G.M., Baroni, C., Kellogg, T.B., 2010a. Constant Holocene Southern-Ocean ^{14}C reservoir ages and ice-shelf flow rates. *Earth Planet. Sci. Lett.* 296, 115–123.
- Hall, B.L., Koffman, T., Denton, G.H., 2010b. Reduced ice extent on the western Antarctic Peninsula at 700–970 cal yr BP. *Geology* 38, 635–638.
- Hambrey, M.J., Glasser, N.F., 2012. Discriminating glacier thermal and dynamic regimes in the sedimentary record. *Sediment. Geol.* 251–252, 1–33.
- Harden, S.L., DeMaster, D.J., Nittrouer, C.A., 1992. Developing sediment geochronologies for high-latitude continental shelf deposits: a radiochemical approach. *Mar. Geol.* 103, 69–97.
- Hass, H.C., Kuhn, G., Monien, P., Brumsack, H.-J., Forwick, M., 2010. Climate fluctuations during the past two millennia as recorded in sediments from Maxwell Bay, South Shetland Islands, West Antarctica. In: Howe, J.A., Austin, W.E.N., Forwick, M., Paetzel, M. (Eds.), *Fjord Systems and Archives*, Geological Society, London, Special Publications, vol. 344, pp. 243–260.
- Heroy, D.C., Anderson, J.B., 2005. Ice-sheet extent of the Antarctic Peninsula region during the Last Glacial Maximum (LGM) – insights from glacial geomorphology. *Geol. Soc. Am. Bull.* 117, 1497–1512.
- Heroy, D.C., Anderson, J.B., 2007. Radiocarbon constraints on Antarctic Peninsula Ice Sheet retreat following the Last Glacial Maximum (LGM). *Quat. Sci. Rev.* 26, 3286–3297.
- Heroy, D.C., Sjunneskog, C., Anderson, J.B., 2008. Holocene climate change in the Bransfield Basin, Antarctic Peninsula: evidence from sediment and diatom analysis. *Antarct. Sci.* 20, 69–87.
- Hillenbrand, C.-D., Larter, R.D., Dowdeswell, J.A., Ehrmann, W., Ó Cofaigh, C., Benetti, S., Graham, A., Grobe, H., 2010a. The sedimentary legacy of a palaeo-ice stream on the shelf of the southern Bellingshausen Sea: clues to West Antarctic glacial history during the Late Quaternary. *Quat. Sci. Rev.* 29, 2741–2763.
- Hillenbrand, C.-D., Smith, J.A., Kuhn, G., Esper, O., Gersonde, R., Larter, R.D., Maher, B., Moreton, S.G., Shimmield, T.M., Korte, M., 2010b. Age assignment of a diatomaceous ooze deposited in the western Amundsen Sea Embayment after the Last Glacial Maximum. *J. Quat. Sci.* 25, 280–295.
- Hillenbrand, C.-D., Bentley, M.J., Stollendor, T., Hein, A.S., Kuhn, G., Graham, A.C.G., Fogwill, C.J., Kristoffersen, Y., Smith, J.A., Anderson, J.B., Larter, R.D., Melles, M., Hodgson, D.A., Mulvaney, R., Sugden, D.E., 2013. Reconstruction of changes in the Weddell Sea sector of the Antarctic Ice Sheet since the Last Glacial Maximum. *Quat. Sci. Rev.* (in press).
- Hjort, C., Ingólfsson, Ó., Möller, P., Lirio, J.M., 1997. Holocene glacial history and sea-level changes on James Ross Island, Antarctic Peninsula. *J. Quat. Sci.* 12, 259–273.
- Hjort, C., Bentley, M.J., Ingólfsson, Ó., 2001. Holocene and pre-Holocene temporary disappearance of the George VI Ice Shelf, Antarctic Peninsula. *Antarct. Sci.* 13, 296–301.
- Hodgson, D.A., 2011. First synchronous retreat of ice shelves marks a new phase of polar deglaciation. *Proc. Natl. Acad. Sci.* 108, 18859–18860.
- Hodgson, D.A., Bentley, M.J., Roberts, S.J., Smith, J.A., Sugden, D.E., Domack, E.W., 2006. Examining Holocene stability of Antarctic Peninsula Ice Shelves. *Eos Trans. Am. Geophys. Union* 87, 305–312.
- Hodgson, D.A., Roberts, S.J., Bentley, M.J., Smith, J.A., Johnson, J.S., Verleyen, E., Vyverman, W., Hodson, A.J., Leng, M.J., Czipersky, A., Fox, A.J., Sanderson, D.C.W., 2009. Exploring former subglacial Hodgson Lake, Antarctica Paper I: site description, geomorphology and limnology. *Quat. Sci. Rev.* 28, 2295–2309.
- Hodgson, D.A., Roberts, S.J., Smith, J.A., Verleyen, E., Sterken, M., Labarque, M., Sabbe, K., Vyverman, W., Allen, C.S., Leng, M.J., Bryant, C., 2013. Late Quaternary environmental changes in Marguerite Bay, Antarctic Peninsula, inferred from lake sediments and raised beaches. *Quat. Sci. Rev.* 68, 216–236.
- Holland, P.R., Jenkins, A., Holland, D.M., 2010. Ice and ocean processes in the Bellingshausen Sea, Antarctica. *J. Geophys. Res.* 115, C05020. <http://dx.doi.org/10.1029/2008JC005219>.
- Holt, T.O., Glasser, N.F., Quincey, D., Siegfried, M.R., 2013. Speedup and fracturing of George VI Ice Shelf, Antarctic Peninsula. *Cryosphere* 7, 797–816.
- Hughes, K.A., Baillie, M.G.L., Bard, E., Beck, J.W., Bertrand, C.J.H., Blackwell, P.G., Buck, C.E., Burr, G.S., Cutler, K.B., Damon, P.E., Edwards, R.L., Fairbanks, R.G., Friedrich, M., Guilderson, T.P., Kromer, B., McCormac, G., Manning, S., Ramsey, C.B., Reimer, P.J., Reimer, R.W., Remmele, S., Southon, J.R., Stuiver, M., Talamo, S., Taylor, F.W., van der Plicht, J., Weyhenmeyer, C.E., 2004. Marine04 marine radiocarbon age calibration, 0–26 cal kyr BP. *Radiocarbon* 46, 1059–1086.
- Huybrechts, P., 2002. Sea-level changes at the LGM from ice-dynamic reconstructions of the Greenland and Antarctic ice sheets during the glacial cycles. *Quat. Sci. Rev.* 21, 203–231.
- Ingólfsson, Ó., Hjort, C., Humlum, O., 2003a. Glacial and climate history of the Antarctic Peninsula since the Last Glacial Maximum. *Arct. Antarct. Alp. Res.* 35, 175–186.
- Ivins, E.R., James, T.S., 2005. Antarctic glacial isostatic adjustment: a new assessment. *Antarct. Sci.* 17, 541–553.
- Jamieson, S., Vieli, A., Livingstone, S.J., Ó Cofaigh, C., Stokes, C.R., Hillenbrand, C.-D., Dowdeswell, J.A., 2012. Ice stream stability on a reverse bed slope. *Nat. Geosci.* 5, 99–802.
- Jamieson, S.S.R., Vieli, A., Ó Cofaigh, C., Stokes, C.R., Livingstone, S.J., Hillenbrand, C.-D., 2014. Understanding controls on rapid ice-stream retreat during the last deglaciation of Marguerite Bay, Antarctica, using a numerical model. *J. Geophys. Res.* 119, 1–17. <http://dx.doi.org/10.1002/2013JF002934>.
- John, B.S., Sugden, D.E., 1971. Raised marine features and phases of glaciation in the South Shetland Islands. *Br. Antarct. Surv. Bull.* 24, 45–111.
- Johnson, J.S., Bentley, M.J., Gohl, K., 2008. First exposure ages from the Amundsen Sea Embayment, West Antarctica: the late Quaternary context for recent thinning of Pine Island, Smith and Pope Glaciers. *Geology* 36, 223–226.
- Johnson, J.S., Smellie, J.L., Nelson, A.E., Stuart, F.M., 2009. History of the Antarctic Peninsula Ice Sheet since the early Pliocene – evidence from cosmogenic dating of Pliocene lavas on James Ross Island, Antarctica. *Glob. Planet. Change* 69, 205–213.
- Johnson, J.S., Bentley, M.J., Roberts, S.J., Binney, S.A., Freeman, S.P., 2011. Holocene deglacial history of the north east Antarctic Peninsula – a review and new chronological constraints. *Quat. Sci. Rev.* 30, 3791–3802.
- Johnson, J.S., Everest, J.D., Leat, P.T., Golledge, N.R., Rood, D.H., Stuart, F.M., 2012. The deglacial history of NW Alexander Island, Antarctica, from surface exposure dating. *Quat. Res.* 77, 273–280.
- Kaiser, J., Lamy, F., Hebbeln, D., 2005. A 70-kyr sea surface temperature record off southern Chile (Ocean Drilling Programme Site 1233). *Paleoceanography* 20, PA4009 [doi:10.1029/2005PA001146](http://dx.doi.org/10.1029/2005PA001146).
- Kennedy, D.S., Anderson, J.B., 1989. Glacial-marine sedimentation and Quaternary glacial history of Marguerite Bay, Antarctic Peninsula. *Quat. Res.* 31, 255–276.
- Khim, B.-K., Yoon, H.I., Kang, C.Y., Bahk, J.J., 2002. Unstable climate oscillations during the late Holocene in the eastern Bransfield Basin, Antarctic Peninsula. *Quat. Res.* 31, 255–276.
- Kilfeather, A.A., Ó Cofaigh, C., Lloyd, J.M., Dowdeswell, J.A., Xu, S., Moreton, S.G., 2011. Ice-stream retreat and ice-sheet history in Marguerite Trough, Antarctic Peninsula: sedimentological and foraminiferal signatures. *Geol. Soc. Am. Bull.* 123, 997–1015.
- King, M.A., Bingham, R.J., Moore, P., Whitehouse, P.L., Bentley, M.J., Milne, G.A., 2012. Lower satellite-gravimetry estimates of Antarctic sea-level contribution. *Nature* 491, 586–589.
- Kunz, M., King, M.A., Mills, J.P., Miller, P.E., Fox, A.J., Vaughan, D.G., Marsh, S.H., 2012. Multi-decadal glacier surface lowering in the Antarctic Peninsula. *Geophys. Res. Lett.* 39, L19502.
- Lal, D., 1991. Cosmic ray labeling of erosion surfaces: in situ nuclide production rates and erosion models. *Earth Planet. Sci. Lett.* 104, 424–439.
- Larter, R.D., Barker, P.F., 1989. Seismic stratigraphy of the Antarctic Peninsula Pacific margin: a record of Pliocene-Pleistocene ice volume and paleoclimate. *Geology* 17, 731–734.
- Larter, R.D., Cunningham, A., 1993. The depositional pattern and distribution of glacial – interglacial sequence on the Antarctic Peninsula Pacific margin. *Mar. Geol.* 109, 203–219.
- Larter, R.D., Vanneste, L.E., 1995. Relict subglacial deltas on the Antarctic Peninsula outer shelf. *Geology* 23, 33–36.
- Larter, R.D., Rebeco, M., Vanneste, L.E., Gamboa, A.P., Barker, P.F., 1997. Cenozoic tectonic, sedimentary and glacial history of the continental shelf west of Graham Land, Antarctic Peninsula. *Antarct. Res. Ser.* 71, 1–27.
- Le Brocq, A.M., Bentley, M.J., Hubbard, A., Fogwill, C.J., Sugden, D.E., Whitehouse, P.L., 2011. Reconstructing the Last Glacial Maximum ice sheet in the Weddell Sea embayment, Antarctica, using numerical modelling constrained by field evidence. *Quat. Sci. Rev.* 30, 2422–2432.
- Li, B., Yoon, H.-I., Park, B.-K., 2000. Foraminiferal assemblages and CaCO_3 dissolution since the last deglaciation in the Maxwell Bay, King George Island, Antarctica. *Mar. Geol.* 169, 239–257.
- Liu, X., Sun, L., Xie, Z., Yin, X., Wang, Y., 2005. A 1300-year record of penguin populations on Ardley Island in the Antarctic, as deduced from the geochemical data in the ornithogenic lake sediments. *Arct. Antarct. Alp. Res.* 37, 490–498.
- Livingstone, S.J., Ó Cofaigh, C., Stokes, C.R., Hillenbrand, C.-D., Vieli, A., Jamieson, S.S.R., 2012. Antarctic palaeo-ice streams. *Earth-Sci. Rev.* 111, 90–128.
- Livingstone, S.J., Ó Cofaigh, C., Stokes, C.R., Hillenbrand, C.-D., Vieli, A., Jamieson, S.R., 2013. Glacial geomorphology of Marguerite Bay palaeo-ice stream, western Antarctic Peninsula. *J. Maps* [doi:10.1080/17445647.2013.829411](http://dx.doi.org/10.1080/17445647.2013.829411).
- Mackintosh, A., White, D., Fink, D., Gore, D.B., Pickard, J., Fanning, P.C., 2007. Exposure ages from mountain dipsticks in Mac. Robertson Land, East Antarctica, indicate little change in ice-sheet thickness since the Last Glacial Maximum. *Geology* 35, 551–554.
- Majewski, W., Wellner, J.S., Szczuciński, W., Anderson, J.B., 2012. Holocene oceanographic and glacial changes recorded in Maxwell Bay, West Antarctica. *Mar. Geol.* 326–328, 67–79.
- Mäusbacher, R., 1991. Die jungquartäre Relief- und Klimageschichte im Bereich der Fildeshalbinsel Süd-Shetland-Inseln, Antarktis (PhD thesis). Universität Heidelberg, 211 p.
- Mäusbacher, R., Müller, J., Schmidt, R., 1989. Evolution of postglacial sedimentation in Antarctic lakes (King George Island). *Z. Geomorphol.* 33, 219–234.
- McKay, R.M., Dunbar, G.B., Naish, T.R., Barrett, P.J., Carter, L., Harper, M., 2008. Retreat history of the Ross Ice Sheet (Shelf) since the Last Glacial Maximum from deep-basin sediment cores around Ross Island. *Paleogeogr. Paleoclimatol. Paleoecol.* 260 (1–2), 245–261.
- Michalchuk, B.R., Anderson, J.B., Wellner, J.S., Manley, P.L., Majewski, W., Bohaty, S., 2009. Holocene climate and glacial history of the northeastern Antarctic Peninsula: the marine sedimentary record from a long SHALDRILL core. *Quat. Sci. Rev.* 28, 3049–3065.

- Milliken, K.T., Anderson, J.B., Wellner, J.S., Bohaty, S.M., Manley, P.L., 2009. High resolution Holocene climate record from Maxwell Bay, South Shetland Islands, Antarctica. *Geol. Soc. Am. Bull.* 121, 1711–1725.
- Minzoni, R.L., Anderson, J.B., Fernandez, R., Wellner, J.S., 2011. Deglacial history and paleoclimatic significance of Herbert Sound, James Ross Island, Antarctic Peninsula. In: 11th ISAES Meeting (Abstract PS12.3), Edinburgh.
- Monien, P., Schnetger, B., Brumsack, H.-J., Hass, H.C., Kuhn, G., 2011. A geochemical record of late Holocene palaeoenvironmental changes at King George Island (maritime Antarctica). *Antarct. Sci.* 23, 255–267.
- Mulvaney, R., Abram, N.J., Hindmarsh, R.C.A., Arrowsmith, C., Fleet, L., Triest, J., Sime, L.C., Alemany, O., Foord, S., 2012. Recent Antarctic Peninsula warming relative to Holocene climate and ice-shelf history. *Nature* 489, 141–144.
- Ó Cofaigh, C., Pudsey, C.J., Dowdeswell, J.A., Morris, P., 2002. Evolution of subglacial bedforms along a paleo-ice stream, Antarctic Peninsula continental shelf. *Geophys. Res. Lett.* 29, 41–1–41–44. <http://dx.doi.org/10.1029/2001GL014488>.
- Ó Cofaigh, C., Dowdeswell, J.A., Allen, C.S., Hiemstra, J., Pudsey, C.J., Evans, J., Evans, D.J.A., 2005. Flow dynamics and till genesis associated with a marine-based Antarctic palaeo-ice stream. *Quat. Sci. Rev.* 24, 709–740.
- Ó Cofaigh, C., Evans, J., Dowdeswell, J.A., Larter, R.D., 2007. Till characteristics, genesis and transport beneath Antarctic palaeo-ice streams. *J. Geophys. Res.* 112, F03006. <http://dx.doi.org/10.1029/2006JF000606>.
- Ó Cofaigh, C., Dowdeswell, J.A., Evans, J., Larter, R.D., 2008. Geological constraints on Antarctic palaeo-ice stream retreat. *Earth Surf. Process. Landf.* 33, 513–525.
- Padman, L., Costa, D.P., Dinniman, M.S., Fricker, H.A., Goebel, M.E., Huckstadt, L.A., Humbert, A., Joughin, I., Lenaerts, J.T.M., Ligtienberg, S.R.M., Scambos, T., van den Broeke, M.R., 2012. Oceanic controls on the mass balance of Wilkins Ice Shelf, Antarctica. *J. Geophys. Res.* 117, C01010. <http://dx.doi.org/10.1029/2011JC007301>.
- Pollard, D., DeConto, R.M., 2012. A simple inverse method for the distribution of basal sliding coefficients under ice sheets, applied to Antarctica. *Cryosphere* 6, 953–971.
- Pope, P.G., Anderson, J.B., 1992. Late Quaternary glacial history of the northern Antarctic Peninsula's western continental shelf: evidence from the marine record. *Antarct. Res. Ser.* 57, 63–91.
- Pritchard, H.D., Vaughan, D.G., 2007. Widespread acceleration of tidewater glaciers on the Antarctic Peninsula. *J. Geophys. Res.* 112 (F03S29), 1–10.
- Pritchard, H.D., Arthern, R.J., Vaughan, D.G., Edwards, L.A., 2009. Extensive dynamic thinning on the margins of the Greenland and Antarctic ice sheets. *Nature* 461, 971–975.
- Pritchard, H.D., Ligtienberg, S.R.M., Fricker, H.A., Vaughan, D.G., van den Broeke, M.R., Padman, L., 2012. Antarctic ice-sheet loss driven by basal melting of ice shelves. *Nature* 484, 502–505.
- Pudsey, C.J., Barker, P.F., Larter, R.D., 1994. Ice sheet retreat from the Antarctic Peninsula shelf. *Cont. Shelf Res.* 14, 1647–1675.
- Pudsey, C.J., Evans, J., 2001. First survey of Antarctic sub-ice shelf sediments reveals Mid-Holocene ice shelf retreat. *Geology* 29, 787–790.
- Pudsey, C.J., Evans, J., Domack, E.W., Morris, P., Del Valle, R.A., 2001. Bathymetry and acoustic facies beneath the former Larsen-A and Prince Gustav ice shelves, north-west Weddell Sea. *Antarct. Sci.* 13, 312–322.
- Pudsey, C.J., Murray, J.W., Appleby, P., Evans, J., 2006. Ice shelf history from petrographic and foraminiferal evidence, northeast Antarctic Peninsula. *Quat. Sci. Rev.* 25, 2357–2379.
- Rabassa, J., 1987. Drumlins and drumlinoid forms in northern James Ross Island, Antarctic Peninsula. In: Menzies, J., Rose, J. (Eds.), *Drumlin Symposium*. Balkema, Rotterdam, pp. 267–288.
- Reimer, P.J., plus 28 others, 2004a. IntCal04 terrestrial radiocarbon age calibration, 0–26 cal kyr BP. *Radiocarbon* 46, 1029–1058.
- Reimer, P.J., Brown, T.A., Reimer, R.W., 2004b. Discussion: reporting and calibration of post-bomb C-14 data. *Radiocarbon* 46, 1299–1304.
- Reimer, P.J., plus 27 others, 2009. IntCal09 and MARINE09 radiocarbon age calibration curves, 0–50,000 years cal BP. *Radiocarbon* 51, 1111–1150.
- Reinardy, B.T.L., Pudsey, C.J., Hillenbrand, C.-D., Murray, T., Evans, J., 2009. Contrasting sources for glacial and interglacial shelf sediments used to interpret changing ice flow directions in the Larsen Basin, Northern Antarctic Peninsula. *Mar. Geol.* 266, 156–171.
- Reinardy, B.T.L., Hiemstra, J., Murray, T., Hillenbrand, C.-D., Larter, R., 2011a. Till genesis at the bed of an Antarctic Peninsula palaeo-ice stream as indicated by micromorphological analysis. *Boreas* 40, 498–517.
- Reinardy, B.T.L., Larter, R.D., Hillenbrand, C.-D., Murray, T., Hiemstra, J.F., Booth, A.D., 2011b. Streaming flow of an Antarctic Peninsula palaeo-ice stream, both by basal sliding and deformation of substrate. *J. Glaciol.* 57, 596–608.
- Rignot, E., Casassa, G., Gogineni, P., Krabill, W., Rivera, A., Thomas, R., 2004. Accelerated ice discharge from the Antarctic Peninsula following the collapse of Larsen B Ice Shelf. *Geophys. Res. Lett.* 31, L18401. <http://dx.doi.org/10.1029/2004GL020697>.
- Rignot, E., Jacobs, S., Mouginot, J., Scheuchl, B., 2013. Ice-shelf melting around Antarctica. *Science* 341, 266–270.
- Rignot, E., Mouginot, J., Scheuchl, B., 2011. Ice flow of the Antarctic Ice Sheet. *Science* 333 (6048), 1427–1430.
- Roberts, S.J., Hodgson, D.A., Bentley, M.J., Sanderson, D.C.W., Milne, G., Smith, J.A., Verleyen, E., Balbo, A., 2009. Holocene relative sea-level change and deglaciation on Alexander Island, Antarctic Peninsula, from elevated lake deltas. *Geomorphology* 112, 122–134.
- Roberts, S.J., Hodgson, D.A., Sterken, M., Whitehouse, P.L., Verleyen, E., Vyverman, W., Sabbe, K., Balbo, A., Bentley, M.J., Moreton, S.G., 2011. Geological constraints on glacio-isostatic adjustment models of relative sea-level change during deglaciation of Prince Gustav Channel, Antarctic Peninsula. *Quat. Sci. Rev.* 30, 3603–3617.
- Rosenheim, B.E., Day, M.B., Domack, E., Schrum, H., Benthien, A., Hayes, J.M., 2008. Antarctic sediment chronology by programmed-temperature pyrolysis: methodology and data treatment. *Geochim. Geophys. Geosyst.* 9 <http://dx.doi.org/10.1029/2007GC001816>.
- Rückamp, M., Braun, M., Suckro, S., Blindow, N., 2011. Observed glacial changes on the King George Island ice cap, Antarctica, in the last decade. *Glob. Planet. Change* 79, 99–109.
- Rutt, I.C., Hagdorn, M., Hulton, N.R.J., Payne, A.J., 2009. The Glimmer community ice sheet model. *J. Geophys. Res.* 114, F02004.
- Royle, J., Sime, L.C., Hodgson, D.A., Convey, P., Griffiths, H., 2013. Differing source water inputs, moderated by evaporative enrichment, determine the contrasting $\delta^{18}\text{O}_{\text{CELLULOSE}}$ signals in maritime Antarctic moss peat banks. *J. Geophys. Res. (Biogeosciences)* 118, 184–194.
- Scambos, T., Hulbe, C., Fahnestock, M., 2003. Climate-induced ice shelf disintegration in the Antarctic Peninsula. In: Domack, E.W., Leverett, A., Burnett, A., Bindshadler, R., Convey, P., Kirby, M. (Eds.), *Antarctic Peninsula Climate Variability: Historical and Palaeoenvironmental Perspectives*, American Geophysical Union, Antarctic Research Series, vol. 79, pp. 79–92. Washington, D.C.
- Scambos, T.A., Bohlander, J.A., Shuman, C.A., Skvarca, P., 2004. Glacier acceleration and thinning after ice shelf collapse in the Larsen B embayment, Antarctica. *Geophys. Res. Lett.* 31, L18402. <http://dx.doi.org/10.1029/2004GL020670>.
- Scambos, T., Fricker, H.A., Cheng-Chien Liu, C.C., Bohlander, J., Fastook, J., Sargent, A., Massom, R., Wu, A.M., 2009. Ice shelf disintegration by plate bending and hydro-fracture: satellite observations and model results of the 2008 Wilkins ice shelf break-ups. *Earth Planet. Sci. Lett.* 280, 51–60.
- Schmidt, R., Mäusbacher, R., Müller, J., 1990. Holocene diatom flora and stratigraphy from sediment cores of two Antarctic lakes (King George Island). *J. Paleolimnol.* 3, 55–74.
- Seong, Y.B., Owen, L.A., Lim, H.S., Yoon, H.I., Kim, Y., Lee, Y.I., Caffee, M.W., 2009. Rate of late Quaternary ice-cap thinning on King George Island, South Shetland Islands, West Antarctica defined by cosmogenic ^{36}Cl surface exposure dating. *Boreas* 38, 207–213.
- Shepherd, A., Ivins, E.R., Geruo, A., Barletta, V.R., Bentley, M.J., Bettadpur, S., Briggs, K.H., Bromwich, D.H., Forsberg, R., Galin, N., Horwath, M., Jacobs, S., Joughin, I., King, M.A., Lenaerts, J.T.M., Li, J., Ligtienberg, S.R.M., Luckman, A., Luthcke, S.B., McMillan, M., Meister, R., Milne, G., Mouginot, J., Muir, A., Nicolas, J.P., Paden, J., Payne, A.J., Pritchard, H., Rignot, E., Rott, H., Sørensen, L.S., Scambos, T.A., Scheuchl, B., Schrama, E.J.O., Smith, B., Sundal, A.V., van Angelen, J.H., van de Berg, W.J., van den Broeke, M.R., Vaughan, D.G., Velicogna, I., Wahr, J., Whitehouse, P.L., Wingham, D.J., Yi, D., Young, D., Zwally, H.J., 2012. A reconciled estimate of Ice-Sheet Mass Balance. *Science* 338 (6111), 1183–1189.
- Shevenell, A.E., Domack, E.W., Kernan, G.M., 1996. Record of Holocene paleoclimate change along the Antarctic Peninsula: evidence from glacial marine sediments, Lallemand Fjord. In: *Papers and Proceedings of the Royal Society of Tasmania* 130, pp. 55–64.
- Sikes, E.L., Samson, C.R., Guilderson, T.P., Howard, W.R., 2000. Old radiocarbon ages in the southwest Pacific Ocean during the Last Glacial Period and deglaciation. *Nature* 405, 555–559.
- Simkins, L.A., Simms, A.R., DeWitt, R., 2013. Relative sea-level history of Marguerite Bay, Antarctic Peninsula derived from optically stimulated luminescence-dated beach cobbles. *Quat. Sci. Rev.* 77, 141–155.
- Simms, A.R., Milliken, K.T., Anderson, J.B., Wellner, J.S., 2011. The marine record of deglaciation of the South Shetland Islands, Antarctica since the Last Glacial Maximum. *Quat. Sci. Rev.* 30, 1583–1601.
- Simms, A.R., Ivins, E.R., DeWitt, R., Kouremenos, P., Simkins, L.M., 2012. Timing of the most recent Neoglacial advance and retreat in the South Shetland Islands, Antarctic Peninsula: insights from raised beaches and Holocene uplift rates. *Quat. Sci. Rev.* 47, 41–55.
- Smith, J.A., Hodgson, D.A., Bentley, M.J., Verleyen, E., Leng, M.J., Roberts, S.J., 2006. Limnology of two Antarctic epishelf lakes and their potential to record periods of ice shelf loss. *J. Paleolimnol.* 35, 373–394.
- Smith, J.A., Bentley, M.J., Hodgson, D.A., Roberts, S.J., Leng, M.J., Lloyd, J.M., Barrett, M.S., Bryant, C., Sugden, D.E., 2007. Oceanic and atmospheric forcing of early Holocene ice shelf retreat, George VI Ice Shelf, Antarctica Peninsula. *Quat. Sci. Rev.* 26, 500–516.
- Smith, J.A., Hillenbrand, C.-D., Pudsey, C.J., Allen, C.S., Graham, A.G.C., 2010. The presence of polynyas in the Weddell Sea during the last glacial period with implications for the reconstruction of sea-ice limits and ice sheet history. *Earth Planet. Sci. Lett.* 296, 287–298.
- Smith, J.A., Hillenbrand, C.-D., Kuhn, G., Larter, R.D., Graham, A.G.C., Ehrmann, W., Moreton, S.G., Forwick, M., 2011. Deglacial history of the West Antarctic Ice Sheet in the western Amundsen Sea Embayment. *Quat. Sci. Rev.* 30, 488–505.
- Smith, R.T., Anderson, J.B., 2010. Ice-sheet evolution in James Ross Basin, Weddell Sea margin of the Antarctic Peninsula: the seismic stratigraphic record. *Geol. Soc. Am. Bull.* 122, 830–842.
- Sterken, M., Roberts, S.J., Hodgson, D.A., Vyverman, W., Balbo, A.L., Sabbe, K., Moreton, S.G., Verleyen, E., 2012. Holocene glacial and climate history of Prince Gustav Channel, northeastern Antarctic Peninsula. *Quat. Sci. Rev.* 31, 93–111.
- Stone, J.O., 2000. Air pressure and cosmogenic isotope production. *J. Geophys. Res.* 105, 23753–23759.

- Stone, J.O., Balco, G.A., Sugden, D.E., Caffee, M.W., Sass, L.C., Cowderly, S.G., Siddoway, C., 2003. Holocene deglaciation of Marie Byrd Land, West Antarctica. *Science* 299, 99–102.
- Stuiver, M., Reimer, P.J., 1993. Extended 14C data base and revised CALIB 3.0 14C age calibration program. *Radiocarbon* 35, 215–230.
- Sugden, D.E., John, B.S., 1973. The ages of glacier fluctuations in the South Shetland Islands, Antarctica. In: van Zinderen Bakker, E.M. (Ed.), *Palaeoecology of Africa of the Surrounding Islands and Antarctica*. International Council of Scientific Unions Scientific Committee on Antarctic Research Conference on Quaternary Studies, A.A. Balkema, Cape Town, pp. 139–159.
- Sugden, D.E., Clapperton, C.M., 1981. An ice-shelf moraine, George VI Sound Antarctica. *Ann. Glaciol.* 2, 135–141.
- Sugden, D.E., Bentley, M.J., Ó Cofaigh, C., 2006. Geological and geomorphological insights into Antarctic Ice Sheet evolution. *Philos. Trans. R. Soc. Ser. A* 364, 1607–1625.
- Tatur, A., del Valle, R., Barczuk, A., 1999. Discussion on the uniform pattern of Holocene tephrachronology in South Shetland Islands, Antarctica. *Polish Polar Studies, XXVI Polar Symposium*, pp. 303–321.
- Thomas, E.R., Marshall, G.J., McConnell, J.R., 2008. A doubling in snow accumulation in the western Antarctic Peninsula since 1850. *Geophys. Res. Lett.* 35, L01706. <http://dx.doi.org/10.1029/2007GL032529>.
- Toro, M., Granados, I., Plaa, S., Giral, S., Antoniadis, D., Galán, L., Martínez Cortizas, A., Soo Lim, H., Appleby, P.G., 2013. Chronostratigraphy of the sedimentary record of Limnopolar Lake, Byers Peninsula, Livingston Island, Antarctica. *Antarct. Sci.* 25, 198–212.
- Turner, J., Colwell, S.R., Marshall, G.J., Lachlan-Cope, T.A., Carelton, A.M., Jones, P.D., Lagun, V., Reid, P.A., Iagovkina, S., 2005. Antarctic climate change during the last 50 years. *Int. J. Climatol.* 25, 279–294.
- Van Beek, P., Reyss, J.-L., Paterne, M., Gersonde, R., Rutgers van der Loeff, M., Kuhn, G., 2002. 226Ra in barite: absolute dating of Holocene Southern Ocean sediments and reconstruction of sea-surface reservoir ages. *Geology* 30, 731–734.
- Vandergoes, M.J., Hogg, A.G., Lowe, D.J., Newnham, R.M., Denton, G.H., Southon, J., Barrell, D.J.A., Wilson, C.J.N., McGlone, M.S., Allan, A.S.R., Almond, P., Petchey, F., Dabell, K., Dieffenbacher-Krall, A.C., Blaauw, M., 2013. A revised age for the Kawakawa/Oruanui tephra, a key marker for the Last Glacial Maximum in New Zealand. *Quat. Sci. Rev.* 74, 195–201.
- Vanneste, L.E., Larter, R.D., 1995. Deep-tow boomer survey on the Antarctic Peninsula Pacific margin: an investigation of the morphology and acoustic characteristics of late Quaternary sedimentary deposits on the outer continental shelf and upper slope. In: Cooper, A.K., Barker, P.F., Brancolini, B. (Eds.), *Geology and Seismic Stratigraphy of the Antarctic Margin*, Antarctic Research Series, vol. 68. American Geophysical Union, Washington D.C., pp. 97–121.
- Vaughan, D.G., Doake, C.S.M., 1996. Recent atmospheric warming and retreat of ice shelves on the Antarctic Peninsula. *Nature* 379, 328–331.
- Vaughan, D.G., Marshall, G.J., Connelly, W.M., Parkinson, C., Mulvaney, R., Hodgson, D.A., King, J.C., Pudsey, C.J., Turner, J., 2003. Recent rapid regional climate warming on the Antarctic Peninsula. *Clim. Change* 60, 243–274.
- Watcham, E.P., Bentley, M.J., Hodgson, D.A., Roberts, S.J., Fretwell, P.T., Lloyd, J.M., Larter, R.D., Whitehouse, P.L., Leng, M.J., Monien, P., Moreton, S.G., 2011. A new Holocene relative sea level curve for the South Shetland Islands, Antarctica. *Quat. Sci. Rev.* 30, 3152–3170.
- Whitehouse, P.L., Bentley, M.J., Le Brocq, A.M., 2012a. A deglacial model for Antarctica: geological constraints and glaciological modelling as a basis for a new model of Antarctic glacial isostatic adjustment. *Quat. Sci. Rev.* 32, 1–24.
- Whitehouse, P.L., Bentley, M.J., Milne, G.A., King, M.A., Thomas, I.D., 2012b. A new glacial isostatic adjustment model for Antarctica: calibrated and tested using observations of relative sea-level change and present-day uplift rates. *Geophys. J. Int.* 190, 1464–1482.
- Willmott, V., Canals, M., Casamor, J.L., 2003. Retreat history of the Gerlache-Boyd Ice Stream, Northern Antarctic Peninsula: an ultra-high resolution acoustic study of the deglacial and post-glacial sediment drape. In: Domack, E.W., Leventer, A., Burnett, A., Bindshadler, R., Convey, P., Kirby, M.E. (Eds.), *Antarctic Peninsula Climate Variability: a Historical and Paleoenvironmental Perspective*, Antarctic Research Series. American Geophysical Union, Washington, DC, pp. 183–194.
- Willmott, V., Domack, E.W., Canals, M., Brachfeld, S., 2006. A high resolution relative paleointensity record from the Gerlache-Boyd paleo-ice stream region, northern Antarctic Peninsula. *Quat. Res.* 66, 1–11.
- Yoo, K.-C., Yoon, H.I., Kim, J.-K., Khim, B.-K., 2009. Sedimentological, geochemical and palaeontological evidence for a neoglacial cold event during the late Holocene in the continental shelf of the northern South Shetland Islands, West Antarctica. *Polar Res.* 28, 177–192.
- Yoon, H.I., Park, B.-K., Kim, Y., Kim, D., 2000. Glaciomarine sedimentation and its paleoceanographic implications along the fjord margins in the South Shetland Islands, Antarctica during the last 6000 years. *Palaeogeogr. Palaeoclimatol. Palaeoecol.* 157, 189–211.
- Yoon, H.I., Park, B.-K., Kim, Y., Kang, C.Y., 2002. Glaciomarine sedimentation and its palaeoclimatic implications on the Antarctic Peninsula shelf over the last 15,000 years. *Palaeogeogr. Palaeoclimatol. Palaeoecol.* 185, 235–254.
- Yoon, H.I., Yoo, K.-C., Park, B.-K., Kim, Y., Khim, B.-K., Kang, C.Y., 2004. The origin of massive diamicton in Marian and Potter Coves, King George Island, West Antarctica. *Geosci. J.* 8, 1–10.
- Zale, R., 1994. ¹⁴C age correction in Antarctic lake sediments inferred from geochemistry. *Radiocarbon* 36, 173–185.
- Zale, R.A., Karlén, W., 1989. Lake sediment cores from the Antarctic Peninsula and surrounding islands. *Geogr. Ann.* 71, 211–220.